UNIVERSITY OF READING

COMPRESSIBLE FLOW IN DUCTS - VARIATIONAL ASPECTS

J. R. WIXCEY

NUMERICAL ANALYSIS REPORT 13/88

DEPARTMENT OF MATHEMATICS

COMPRESSIBLE FLOW IN DUCTS - VARIATIONAL ASPECTS

J. R. WIXCEY

NUMERICAL ANALYSIS REPORT 13/88

Department of Mathematics
P.O. Box 220
University of Reading
Whiteknights
Reading
RG6 2AX
United Kingdom

This work forms part of the research programme of the Institute of Computational Fluid Dynamics at the Universities of Oxford and Reading and has been supported by the S.E.R.C.

CONTENTS

ABSTRACT

This report continues the work by the author on duct flow initiated in [4]. A quasi one-dimensional finite element method on a fixed grid is derived from a stationary principle. The numerical method is formulated first on a uniform grid and the graphical results presented. On consideration of the relative accuracy of this approach an algorithm is stated for the definition of an appropriate irregular grid and the subsequent solution on it used to illustrate the possible improvements that may result.

ACKNOWLEDGEMENTS

I would like to thank Dr. M.J. Baines and Dr. D. Porter for their guidance in this work.

I acknowledge an S.E.R.C. research studentship.

INTRODUCTION

An introduction to duct flow and its approximate parameterization is presented in [4].

The aim here is to formulate a numerical method for the approximate solution of quasi one-dimensional duct flow through the derivation of a stationary principle.

In Section One the properties of the general compressible flow to be considered, together with the one-dimensional form of the motion equations, are presented. A brief resume of the quasi one-dimensional approximation to duct flow is given (see [4]) with the associated revised equations of motion.

In Section Two two stationary principles equivalent to the conditions defining quasi one-dimensional duct flow are derived. The first, it is shown, may be obtained from a known stationary principle for three dimensional flow and the second, which is peculiar to quasi one-dimensional duct flow, is used to develop a numerical finite element method.

The finite element method is implemented, for various duct types, on a uniform fixed grid in Section Three and comparison made between this and the algebraic formulation of [4].

In Section Four the effect of grid definition on the accuracy of the numerical method is considered. A simple algorithm for the definition of a fixed irregular grid is presented, together with the associated benefits of this approach.

SECTION ONE : QUASI ONE-DIMENSIONAL DUCT FLOW

In this section the properties of a general compressible flow are presented together with the one-dimensional form of the equations of motion. A quasi one-dimensional approximation to duct flow is then introduced (for a more comprehensive review see [4]), which is a particular example of compressible flow, and the revised associated motion equations stated.

1.1 COMPRESSIBLE FLOW PROPERTIES

The compressible fluid to be considered is modelled by the polytropic gas with the flow having the properties that it is inviscid and steady. It is therefore characterised by streamlines in the flow field on which the entropy, S, is constant (see [1]).

The fluid itself satisfies the law of Boyle and Gay-Lussac,

$$p\,\nu = \left[R_o/m \right] T \ , \tag{1.1}$$

where p represents pressure, R_o is the universal gas constant, m the molecular weight of the gas, T the temperature and ν the specific volume defined by

$$\nu = 1/\rho \ , \tag{1.2}$$

where ρ is density. The fluid motion is governed by the conservation

equations of fluid dynamics, which in the present circumstances are

$$\text{CONSERVATION OF MASS} : \qquad \underline{\nabla}.(\rho\ \underline{v}) = 0\ , \qquad (1.3)$$

$$\text{CONSERVATION OF MOMENTUM} : \qquad \underline{\nabla}\ p + \rho\ (\underline{v}.\underline{\nabla})\ \underline{v} = 0\ , \qquad (1.4)$$

$$\text{CONSERVATION OF ENERGY} : \qquad \underline{v}.\underline{\nabla}\ S = 0\ , \qquad (1.5)$$

where $\underline{v}$ denotes the fluid velocity and $\underline{\nabla}$ the gradient operator, together with the appropriate equation of state

$$\text{ENTROPIC EQUATION OF STATE} : \quad p = \eta\ \rho^{\gamma}\ , \qquad (1.6)$$

where η is a function of entropy and γ is the adiabatic exponent associated with the fluid.

Additional variables associated with the flow are mass flow, $\underline{Q}$, and flow stress, P, related to those already stated by

$$\underline{Q} = \rho\ \underline{v} \qquad (1.7)$$

and

$$P = p + \rho\ (\underline{v}.\underline{v})\ . \qquad (1.8)$$

Pressure gradients

The pressure, density, temperature and entropy associated with a particle in any motion of such a compressible inviscid gas are related by an enthalpy function $\aleph(S,p)$ (see [2]) with gradients:

$$\frac{\partial \aleph}{\partial S} = T \quad ; \quad \frac{\partial \aleph}{\partial p} = \nu\ . \qquad (1.9)$$

This enthalpy function has a unique inverse for a given entropy value, since $\nu > 0$, and therefore a pressure valued function may be defined in the present case of a polytropic gas by

$$p[\aleph,S] = \eta^{(1/(1-\gamma))} \left[[(\gamma-1)/\gamma]\ \aleph \right]^{(\gamma/(\gamma-1))} , \qquad (1.10)$$

with associated gradients:

$$\frac{\partial p}{\partial \aleph} = \rho \quad ; \quad \frac{\partial p}{\partial S} = - \rho\ T . \qquad (1.11)$$

The total energy of the particle at any instant of a motion, h, is now introduced as a function of the enthalpy and fluid speed,

$$h = \aleph + ((\underline{v}.\underline{v})/2) , \qquad (1.12)$$

and substitution into (1.10) yields a pressure function now of three arguments, namely

$$p[\underline{v},h,S] = \eta^{(1/(1-\gamma))} \left[[(\gamma-1)/\gamma]\ [h-((\underline{v}.\underline{v})/2)] \right]^{(\gamma/(\gamma-1))} . \qquad (1.13)$$

The gradients of this function are,

$$\frac{\partial p}{\partial \underline{v}} = - \rho\ \underline{v} \quad , \quad \frac{\partial p}{\partial h} = \rho \quad , \quad \frac{dp}{\partial S} = - \rho\ T , \qquad (1.14)$$

and it is the first of these, i.e. that with respect to fluid speed, which is required for the coming work.

Additional flow properties

The properties of the flow are now reconsidered with the inclusion of several simplifying features; the flow is firstly assumed to be homentropic so that the entropy is constant, not only on a streamline, but throughout the flow field except at discontinuities such as shocks. The equation (1.5) is therefore satisfied identically. The flow is also assumed to be irrotational, i.e.

$$\underline{\nabla} \times \underline{v} = \underline{0} \ . \tag{1.15}$$

This equality is satisfied by the introduction of a velocity potential, ϕ, such that

$$\underline{v} = \underline{\nabla} \phi \ . \tag{1.16}$$

The flow can now be thought of as being homenergic so that the total energy (1.12) is constant in the flow field, as can be seen from the alternative form of the conservation of momentum equation

$$\underline{\nabla} h - T \underline{\nabla} S = \underline{v} \times (\underline{\nabla} \times \underline{v}) \ , \tag{1.17}$$

(see [3]). The motion equations of the flow reduce to (1.3) together with the irrotationality condition (1.16).

In the present case interest lies with one-dimensional flow, which of necessity is irrotational. The appropriate one-dimensional form of the irrotationality condition therefore becomes redundant and is no longer a necessary flow condition. The flow is completely defined by the constant values of entropy and total energy in the flow field and the conservation of mass equation

$$\frac{d}{dx}(\rho v) = 0 \ . \tag{1.18}$$

It now only remains to define the particular gas flow to be considered in terms of the thermodynamic constants associated with the fluid, which in the present case is taken to be air, as specified in [3], namely

$$\begin{aligned} \gamma &= 1.4 \ , \\ R_o &= 8.31 \ \text{Jmol}^{-1}\text{K}^{-1} \ , \\ m &= 28.96 \times 10^{-2} \ \text{kg} \ , \end{aligned} \tag{1.19}$$

and also the flow constants resulting from the homenergic and homentropic nature of the flow (see [3])

$$\begin{aligned} h &= 2.74 \times 10^{5} \ \text{Jmol}^{-1}\text{kg}^{-1} \ , \\ \eta &= 7.08 \times 10^{4} \ \text{(SI UNITS)} \ . \end{aligned} \tag{1.20}$$

1.2 DUCT FLOW

The analysis is now confined to a specific example of compressible flow through various forms of duct. The ducts considered are firstly converging or diverging axi-symmetric cone sections and then as a combination of these the more complex axi-symmetric de-Laval nozzle (see [4]).

The duct flow field may be thought of as consisting of streamlines invariant in time. The full duct flow may be reduced to the consideration of conditions on a single representative streamline on which, on average, the fluid particle history typifies the full flow (see [5]).

In the present work the duct is supposed to be slowly varying so that, to a first approximation, the motion is one-dimensional in the x-direction only. Then the flow must be irrotational and therefore by now assuming that the flow is homentropic it must also be homenergic. The streamlines in the flow field are consequently indistinguishable and each of them may be thought of as the representative streamline, defined by the constant specified values of entropy and total energy (1.20).

The conservation of mass equation appropriate to quasi one-dimensional primary duct flow is

$$\frac{d}{dx}(Q(x)\,A(x)) = 0\ , \tag{1.21}$$

where $A(x)$ is the local cross-sectional area of the duct and $Q(x)$ is

the local mass flow defined by (1.7) which it is convenient to restate as,

$$Q = \rho v \ . \qquad (1.22)$$

The complete solution of the flow, in which all of the flow variables are recovered, is possible on using the total energy equation (1.12) in an appropriate form. This form may be obtained on writing the enthalpy term in (1.12) as a function of density by equating (1.10) and the equation of state (1.6). Note that the particular form of (1.6) associated with the fluid is obtained by substitution of (1.19a) and (1.20b).

The quasi one-dimensional approximation to duct flow is therefore defined by the constant values of entropy and total energy (1.20) together with the conservation of mass equation (1.21) and the mass flow condition (1.7). It is these equations that must be satisfied for complete solution of the approximate flow.

SECTION TWO : TWO REPRESENTATIVE STATIONARY PRINCIPLES OF QUASI ONE-DIMENSIONAL DUCT FLOW

It is possible to derive several stationary principles equivalent to the conditions defining quasi one-dimensional duct flow. In this section two such stationary principles are considered; the first, it is shown, may be obtained from a known stationary principle for three dimensional flow. The second is peculiar to quasi one-dimensional flow and is the more convenient one from which to develop a numerical method for the approximate fluid speed in a duct motion.

2.1 A STATIONARY PRINCIPLE FOR QUASI ONE-DIMENSIONAL DUCT FLOW

The quasi one-dimensional approximation to duct flow is defined by (1.21) and (1.22) which are considered to hold in a fixed domain, D, which represents the duct axis. Let ξ be an undetermined function of position and define a functional $I = I(\underline{z})$ by

$$I = \int_D [\, Q\, A\, v + A\, p(v) - Q\, A\, \frac{d(\xi)}{dx} \,]\, dx \,, \qquad (2.1)$$

where

$$\underline{z} = (\, Q \,,\, v \,,\, \xi \,) \,, \qquad (2.2)$$

and $A = A(x)$ is the specified duct area variation at position x. The function $p(v)$ in (2.1) is that defined by (1.13) where in one dimension $\underline{v}.\underline{v} \equiv v^2$ and the arguments h and S have now been omitted as in this case they take constant values.

Now consider small, arbitrary variations of the arguments (2.2) applied at every point, x, of the domain

$$\delta \underline{z} = (\delta Q , \delta v , \delta \xi) . \tag{2.3}$$

The functional (2.1) is stationary with respect to the variations (2.3) if and only if its first variation is zero, that is,

$$\delta I = \delta \left[\int_D [Q A v + A p(v) - Q A \frac{d(\xi)}{dx}] dx \right] = 0, \tag{2.4}$$

which may be written explicitly as

$$\delta I = \int_D [\delta Q \left[A v - A \frac{d\xi}{dx} \right] + \delta v \left[Q A + A \frac{dp}{dv} \right] + \delta \xi \left[\frac{d}{dx} (Q A) \right]] dx = 0 , \tag{2.5}$$

where at the ends of the domain it is assumed that $\delta \xi = 0$.

Then from the fundamental lemma of calculus of variations (see [6]) if δI is zero for arbitrary variations (2.3) then the individual components of the integrand in the expression (2.5) are zero. Thus the Euler-Lagrange differential equations of the stationary principle (2.4), i.e. the natural conditions, are given by

$$\delta Q \; : \; v = \frac{d\xi}{dx} \; , \tag{2.6}$$

$$\delta v \; : \; Q = - \frac{dp}{dv} \tag{2.7}$$

and

$$\delta \xi \; : \; \frac{d}{dx} (Q\,A) = 0 \; . \tag{2.8}$$

The natural condition (2.7) may be written in the form

$$Q = \rho \, v \; , \tag{2.9}$$

by using (1.14a). It can now be seen that (2.8) is the conservation of mass equation (1.21) particular to quasi one-dimensional duct flow and (2.9) is exactly the definition of mass flow (1.22). Condition (2.6) may be identified as a trivial reduction in one dimension of the irrotationality condition (1.16) but, as stated previously, it plays no part in the definition of the flow. The values of ξ throughout the flow may of course be computed by integration of (2.6) but these are of no physical interest.

Therefore the generating functional (2.1) is stationary with respect to first variations of its arguments if the original problem, in the present case expressed by (1.21) and (1.22), is satisfied; this also being true conversely. Thus making the functional (2.1) stationary is equivalent to satisfying the differential equations associated with the particular problem we are considering and it therefore determines the quasi one-dimensional approximation to the duct flow problem.

It will now be shown that the functional (2.1), and thus the stationary principle (2.4), may also be obtained from a functional found in [2], namely

$$S = \int_V [\ \underline{Q}.\underline{v} + p(\underline{v}) - \underline{Q}.\underline{\nabla}\ \phi\ ]\ dV\ , \tag{2.10}$$

where V is a closed simply connected region and $p(\underline{v})$ is the function used in (2.1). The natural conditions of the stationary principle $\delta S = 0$ are the equations governing a full compressible, homentropic, irrotational (and therefore homenergic) flow (see (1.3) and (1.16)), that is

$$\underline{\nabla}.\underline{Q} = 0\ , \tag{2.11}$$

$$\underline{Q} = \rho\ \underline{v}\ , \tag{2.12}$$

and

$$\underline{v} = \underline{\nabla}\ \phi\ . \tag{2.13}$$

In cartesian co-ordinates (2.10) is

$$S = \iiint_V [\ \underline{Q}.\underline{v} + p(\underline{v}) - \underline{Q}.\underline{\nabla}\ \phi\ ]\ dx\ dy\ dz\ , \tag{2.14}$$

where integration is over the three dimensional domain V and $\underline{\nabla}$ is the cartesian gradient operator (in three dimensions). (2.14) may be put into a form more applicable to duct flow by making a co-ordinate change to cylindrical polar co-ordinates to give

$$S = \iiint_V [\ \underline{Q}.\underline{v} + p(\underline{v}) - \underline{Q}.\underline{\nabla}\ \phi\ ]\ dx\ r dr\ d\theta\ , \qquad (2.15)$$

where the domain V may now be thought of as representing the duct itself; the gradient operator now takes the form,

$$\underline{\nabla}\ \phi = \frac{\partial \phi}{\partial r}\ \hat{\underline{u}}_r + \frac{1}{r}\ \frac{\partial \phi}{\partial \theta}\ \hat{\underline{u}}_\theta + \frac{\partial \phi}{\partial x}\ \hat{\underline{u}}_x\ , \qquad (2.16)$$

where $\hat{\underline{u}}_r$, $\hat{\underline{u}}_\theta$ and $\hat{\underline{u}}_x$ are unit vectors in the directions of increasing r, θ and x.

Since the duct is axi-symmetric, (2.15) simplifies to

$$S = 2\ \pi \iint_\sigma [\ \underline{Q}.\underline{v} + p(\underline{v}) - \underline{Q}.\underline{\nabla}\ \phi\ ]\ dx\ r dr\ . \qquad (2.17)$$

where σ is that part of the surface $\theta = 0$ lying within V. Consistent with the assumptions of quasi one-dimensional flow the arguments of the functional (2.17) are now supposed, to a first approximation, to be dependent only on x. Thus,

$$S = \int_D [\ Q\ v + p - Q\ \frac{d\phi}{dx}\ ]\ \pi\ R^2\ dx\ , \qquad (2.18)$$

where the domain D represents the duct axis and R = R(x) the radial distance from the axis to the duct wall at position x. This may be written in the form of (2.1),

$$S = \int_D [\ Q\ v + p - Q\ \frac{d\phi}{dx}\ ]\ A(x)\ dx\ , \qquad (2.19)$$

where now ϕ takes on the same passive role as ξ in (2.1) ,since the local cross-sectional area of the duct is given by

$$A(x) = \pi R^2 \ . \tag{2.20}$$

2.2 ANOTHER STATIONARY PRINCIPLE FOR QUASI ONE-DIMENSIONAL DUCT FLOW

The equations (1.21) and (1.22) are again considered to hold in the same fixed domain, D, representing the duct axis. In the present case let ψ be an undetermined function of position and define a further functional $J = J(\underline{z})$

$$J = \int_D [\ Q\ v + p(v) + \psi \frac{d\ (Q\ A)}{dx}\ ]\ dx\ , \tag{2.21}$$

with arguments,

$$\underline{z} = (\ Q\ ,\ v\ ,\ \psi\ )\ . \tag{2.22}$$

Now consider small, arbitrary variations of the arguments applied at every point, x, of the domain

$$\delta\underline{z} = (\ \delta Q\ ,\ \delta v\ ,\ \delta\psi\ )\ . \tag{2.23}$$

The functional (2.21) is stationary with respect to the variations (2.23) if and only if its first variation is zero so that

$$\delta J = \delta \left[\int_D [\ Q\ v + p(v) + \psi \frac{d\ (Q\ A)}{dx}\ ]\ dx \right] = 0, \tag{2.24}$$

which may be written as,

$$\delta J = \int_D \left[\delta Q \left[v - A \frac{d\phi}{dx} \right] + \delta v \left[Q + \frac{dp}{dv} \right] + \delta \phi \left[\frac{d}{dx} (Q A) \right] \right] dx = 0 \ , \tag{2.25}$$

where at the ends of the domain it is assumed that $\delta\phi = 0$. Then the natural conditions of the stationary principle (2.24) are given by

$$\delta Q \ : \ v = A \frac{d\phi}{dx} \ , \tag{2.26}$$

$$\delta v \ : \ Q = \rho \, v \tag{2.27}$$

and

$$\delta \phi \ : \ \frac{d}{dx} (Q A) = 0 \ , \tag{2.28}$$

where (2.27) is again obtained by the substitution of (1.14a). It may now be seen that (2.27) and (2.28) are exactly the equations defining quasi one-dimensional duct flow ((1.22) and (1.21) respectively). Condition (2.26) again plays no part in the definition of the flow but the value of ϕ throughout may be determined by the integration of (2.26). Therefore making the functional (2.21) stationary is also equivalent to satisfying the differential equations associated with the quasi one-dimensional approximation to the flow problem under consideration.

The natural condition (2.28) may be imposed as a constraint on the variations in (2.24) on ensuring that mass conservation is satisfied by assigning

$$Q(x)\ A(x) = \text{CONSTANT} \ , \tag{2.29}$$

which in the present case is chosen (see [4]) such that,

$$Q(x) = \frac{C\ A_e}{A(x)} \ , \tag{2.30}$$

where C is the mass flow rate entry value to the central streamline along the duct axis and A_e is the duct entry surface area. This gives a local map (2.30) on the central streamline between distance along the duct axis, x, and the local mass flow rate, Q(x).

The flow boundaries are a pair of points on the central streamline at the inlet and outlet duct locations and the boundary conditions, analagous to those for the full flow (see [5]), are the assignment of mass flow rates at entry, Q_e,

$$Q_e = C \ , \tag{2.31}$$

and by using the relationship (2.30) at outlet, Q_o,

$$Q_o = \frac{C\ A_e}{A_o} \ , \tag{2.32}$$

where A_o is the outlet duct cross-sectional area.

The remaining natural conditions (2.26) and (2.27) are those associated with the new stationary principle,

$$\delta K = \delta \left[\int_D \left(\frac{C A_e}{A(x)} v + p(v) \right) dx \right] = 0 , \qquad (2.33)$$

where $K = K(v)$. The principle $\delta K = 0$ may be applied to a particular duct motion on prescription of the the overall duct area variation, the associated entry mass flow rate to the central streamline (2.31), the entry duct area and the constant values of entropy and total energy. The stationary values of (2.33) are exactly the same as those for (2.24) and the solution obtained for the approximation to the actual flow is the same (see [6]).

Note that K depends only on the fluid speed and therefore the principle (2.33) can now readily be used in the development of a numerical method for the derivation of the approximate fluid speed throughout a particular duct motion.

2.3 A NUMERICAL FORMULATION OF QUASI ONE-DIMENSIONAL DUCT FLOW

In the absence of shocks the fluid speed is continuous throughout the duct; a semi-discrete approximation to the fluid speed is now sought of the form

$$\bar{v} = \sum_{i=1}^{N} a_i \, \alpha_i(x) \ , \tag{2.34}$$

in a subspace of C^0, where a_i, $i = 1(1)N$, are constant coefficients and $\alpha_i = \alpha_i(x)$, $i = 1(1)N$, are test functions spanning C^0.

The substitution of the approximation (2.34) into the functional K, underlying the stationary principle (2.33), yields now a function, L, of the unknown coefficients a_i,

$$L = L(a_1, a_2, \ldots , a_{N-1}, a_N) \ , \tag{2.35}$$

where $L = K(\bar{v})$ is defined by,

$$L = \int_D \left[\frac{C \, A_e}{A(x)} \, \bar{v} + p(\bar{v}) \right] dx \ , \tag{2.36}$$

on the same domain, D, as its counterpart in continuous space. Therefore making the function (2.36) stationary gives an approximation to the stationary point of the functional K in the chosen subspace; the condition for this is simply

$$\frac{\partial L}{\partial a_i} = 0 \ . \qquad [\ i = 1(1)N \ ] \tag{2.37}$$

The explicit form of (2.37) is therefore obtained by differentiation of the function (2.36), i.e.

$$\frac{\partial L}{\partial a_i} = \int_D \left[\frac{C\, A_e}{A(x)} \frac{\partial}{\partial a_i}(\bar{v}) + \frac{\partial}{\partial a_i}(p(\bar{v})) \right] dx \,. \quad [\, i = 1(1)N \,] \tag{2.38}$$

[a] [b]

The two steps in this evaluation, by substitution of the pressure gradient (1.14a), are

$$[a] \;:\; \frac{\partial}{\partial a_i}(\bar{v}) = \alpha_i \quad [\, i = 1(1)N \,]$$

and (2.39)

$$[b] \;:\; \frac{\partial}{\partial a_i}(p(\bar{v})) = \frac{\partial \bar{v}}{\partial a_i} p'(\bar{v}) = -\alpha_i \bar{v} \rho(\bar{v}) \,. \quad [\, i = 1(1)N \,]$$

The aim ultimately being to derive the approximate fluid speed throughout the duct, this necessitates that the density term in [b] be replaced by an algebraic relation between these two flow variables (see [3]), which is

$$\rho(\bar{v}) = \eta^{(1/(1-\gamma))} \left[[(\gamma-1)/\gamma] [h-(\bar{v}^2/2)] \right]^{(1/(\gamma-1))} , \tag{2.40}$$

where the flow constants take the prescribed values (1.19a) and (1.20).

The conditions (2.37) now take the form of a system of non-linear equations, the unknown quantities being the coefficients, a_i:

$$\int_D \left[\frac{C\,A_e}{A(x)} - \bar{v}\,\eta^{(1/(1-\gamma))} \left[\frac{(\gamma-1)}{\gamma} \left(h - \left(\frac{\bar{v}}{2} \right)^2 \right) \right]^{(1/(\gamma-1))} \right] \alpha_i \, dx = 0 \,, \quad [\, i = 1(1)N \,] \tag{2.41}$$

where we recall that $\bar{v}$ is the piecewise linear approximation to the fluid speed (2.34).

The system (2.41) may now be written in terms of an inner-product,

$$\left\langle \frac{C\,A_e}{A(x)} - \rho\,\bar{v} \,,\, \alpha_i \right\rangle = 0 \,, \quad i = 1(1)N \,, \tag{2.42}$$

where $\langle \cdot \,,\, \cdot \rangle$ denotes integration over the domain and it may be noted, by using (2.30), that subsequent to the specification of the test functions, α_i, (2.42) is a particular weak form of the mass flow condition (1.22).

On solution of this system (2.42) the function (2.36) has been made stationary with respect to its arguments, solving the given flow problem discretely using Galerkin's method (see [7]), and thus determining an approximation to the axial fluid speed throughout a particular duct motion.

2.4 SYSTEM SOLUTION ALGORITHM

In the present case the test functions are chosen to be piecewise linear basis functions of local compact support. A typical interior basis function is illustrated in FIG.1 and defined by,

$$\alpha_i = \begin{cases} \dfrac{x - S_{i-1}}{S_i - S_{i-1}} & S_{i-1} \le x \le S_i \quad (\alpha_i^1) \\ \dfrac{S_{i+1} - x}{S_{i+1} - S_i} & S_i \le x \le S_{i+1} \quad (\alpha_i^2) \end{cases} \qquad [\, i = 2(1)N-1 \,] \,, \quad (2.43)$$

α_i being zero outside the interval $[\, S_{i-1} \,,\, S_{i+1} \,]$. The coefficients a_i, $i = 1(1)N$, in (2.34) may now be interpreted as the unknown nodal values at the fixed nodal positions S_i, $i = 1(1)N$, to be specified, in the solution domain.

FIG.1

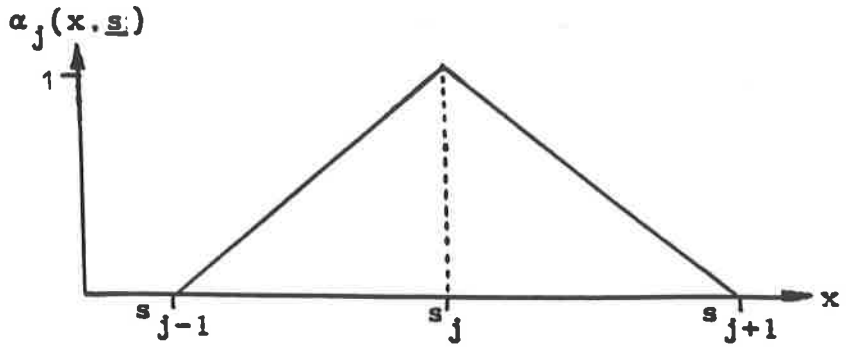

Numerical quadrature

In the system of equations (2.42) the integrals are evaluated by performing the required integration numerically using a quadrature formula. Note that the integrands are zero everywhere except over small domains spanning two elements

$$e_{i-1} = [\, S_{i-1} \,,\, S_i \,]$$

and (2.44)

$$e_i = [\, S_i \,,\, S_{i+1} \,] \,.$$

Therefore denoting by G the integrand of the i'th equation of (2.42) for an interior node the integration may be written in two parts, namely

$$\int_{S_{i-1}}^{S_i} G\, \alpha_i^1 \, dx + \int_{S_i}^{S_{i+1}} G\, \alpha_i^2 \, dx = 0 \qquad i = 2(1)N-1 \,, \tag{2.45}$$

inferred from the interior basis function definition (2.43).

The quadrature formula applied in the present case, to each of the integrals in (2.45), is the closed three-point Newton-Cotes formula more commonly known as Simpson's Rule. This is defined on a general domain [a,b] by

$$\int_b^a f(x)\, dx = \left[\frac{b-a}{6} \right] \left[f(b) + 4f\left(\frac{a+b}{2} \right) + f(a) \right] . \tag{2.46}$$

Iterative method

The unknown nodal amplitudes, a_i, at the associated nodal positions, S_i, are now obtained by simultaneous solution of the equation system (2.42), by application of an iterative method.

Define first a vector of the unknown coefficients

$$\underline{a} = (a_1 , a_2 , \quad , a_N)^T , \tag{2.47}$$

and consider also the non-linear system of equations (2.42) written in vector form

$$\underline{F} = (f_1 , f_2 , \quad , f_N)^T = \underline{0} , \tag{2.48}$$

where

$$f_i(\underline{a}) = f_i(a_1 , a_2 , \quad , a_N) \quad [i = 1(1)N] . \tag{2.49}$$

Now a general iterative method may be defined by

$$\underline{a}^{j+1} = \underline{g}(\underline{a}^j) , \tag{2.50}$$

where $\underline{a}^{j+1}$ is the updated solution vector at iteration level j+1 and g is a function of $\underline{a}^j$, the present solution vector at iteration level j. The exact fixed point of the system (2.50), a^*, if it exists, then satisfies,

$$\underline{a}^* = \underline{g}(\underline{a}^*) , \tag{2.51}$$

which may be found approximately if $\underline{a}^{j+1} = \underline{a}^j$ to within a specified tolerance.

The system $\underline{F} = \underline{0}$ may be solved by this iterative process by making a suitable choice of $\underline{g}$; thus in the present case Newton's iterative method for several variables is employed whence $\underline{g}$ takes the particular form

$$\underline{g}(\underline{a}^j) = \underline{a}^j - [\, J(\underline{a}^j)\,]^{-1}\, \underline{F}(\underline{a}^j)\ , \tag{2.52}$$

where the Jacobian matrix of the system J, with its (n,m) th entry denoted

$$a_{n,m} = \frac{\partial f_n(\underline{a})}{\partial a_m}\ , \tag{2.53}$$

is defined by

$$J(\underline{a}^j) = \left[\frac{\partial f_n(\underline{a})}{\partial a_m} \Big|_{\underline{a} = \underline{a}^j} \right] \qquad \begin{matrix} n = 1(1)N\ , \\ m = 1(1)N \end{matrix} \tag{2.54}$$

in which case the fixed point of (2.52) satisfies

$$\underline{F}(\underline{a}^*) = \underline{0}\ . \tag{2.55}$$

The dimension of the Jacobian matrix in the iterative method is obviously dependent on the number of equations in the system and thus on the number of nodes in the numerical formulation. Assuming there to be at least two interior nodes, i.e.

$$N \geq 4\ , \tag{2.56}$$

then inversion of the Jacobian matrix necessary for (2.52) will be non-trivial. The iterative method is therefore actually used in an equivalent form by solving the linear system

$$J(\underline{a}^j)\ \underline{z}^{j+1} = -\ \underline{F}(\underline{a}^j)\ , \tag{2.57}$$

for the solution updates and then updating by

$$\underline{a}^{j+1} = \underline{a}^j + \underline{z}^{j+1}\ . \tag{2.58}$$

The interative scheme here is said to have converged when the pointwise maximum residual error of the system of equations is less than a specified tolerance,

$$\text{MAX}\ \left|\ f_i(\underline{a}^j)\ \right| < 0.00001\ , \tag{2.59}$$

which is an alternative condition to that stated earlier.

SECTION THREE : IMPLEMENTATION OF THE NUMERICAL METHOD ON A UNIFORM GRID

3.1 FORMULATION

The solution domain, in which the defining equations ((1.21) and (1.22)) of quasi one-dimensional duct flow hold, is defined as

$$0.0 \leq x \leq d \ , \tag{3.1}$$

where d is the domain length. The numerical solution grid (see FIG.2) is specified such that the boundary nodal positions, S_1 and S_N, lie at the domain extremes

$$\begin{aligned} S_1 &= 0.0 \ , \\ S_N &= d \ , \end{aligned} \tag{3.2}$$

where N is the number of nodes in the numerical formulation. The interior nodal positions are equi-spaced by the distance H where

$$H = (d \ / \ N) \ , \tag{3.3}$$

which is therefore the constant element length (see (2.44)) throughout so that

$$S_{i+1} - S_i = H \qquad [\ i = 1(1)N-1 \ ] \ . \tag{3.4}$$

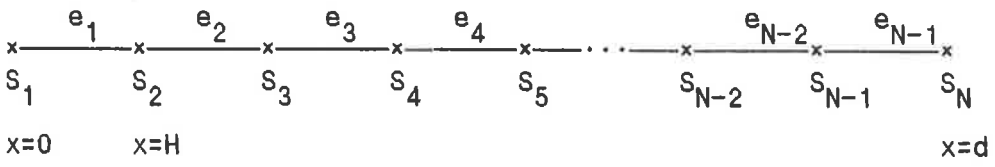

FIG TWO

The piece-wise linear basis functions associated with an interior node in the present formulation take the simplified form,

$$\alpha_i = \begin{cases} + \dfrac{x}{H} - (i-2) & (i-2)H \leq x \leq (i-1)H \quad (\alpha_i^1) \\ \\ - \dfrac{x}{H} + i & (i-1)H \leq x \leq iH \quad (\alpha_i^2) \ , \end{cases} \qquad [\ i = 2(1)N-1\ ] \qquad (3.5)$$

uniform in i, and for the boundary nodes the basis functions are defined by

$$\alpha_1 = - \frac{x}{H} + 1 \qquad 0 \leq x \leq H$$

and (3.6)

$$\alpha_N = \frac{x}{H} - (N-2) \qquad (N-2)H \leq x \leq (N-1)H \ .$$

The corresponding approximation to the fluid speed, and thus of the discrete function L (2.36), is obtained by substituting (3.5) and (3.6) into (2.34); making this function stationary produces the relevant equation system.

Evaluation of the integrals in the system by the numerical quadrature (2.46) then yields a particular non-linear system of equations for the unknown nodal amplitudes, applicable to the uniform fixed grid formulation, namely,

$$f_1(\underline{a}) = \frac{CA_e}{6} H \left[\frac{1}{A_e} + \frac{2}{A(H/2)} \right]$$

$$- \beta \frac{H}{6} \left[a_1 (h - \frac{a_1^2}{2})^{5/2} + (a_1 + a_2) (h - (\frac{a_1 + a_2}{8})^2)^{5/2} \right] = 0$$

$$f_1(\underline{a}) = \frac{CA_e}{6} H \left[\frac{2}{A((2i-3)H/2)} + \frac{2}{A((2i-2)H/2)} + \frac{2}{A((2i-1)H/2)} \right]$$

$$- \beta \frac{H}{6} \left[2a_1 (h - \frac{a_1^2}{2})^{5/2} + (a_{i-1} + a_i) (h - (\frac{a_{i-1} + a_i}{8})^2)^{5/2} \right.$$

$$\left. + (a_1 + a_{i+1}) (h - (\frac{a_i + a_{i+1}}{8})^2)^{5/2} \right] = 0 \quad [\, i = 2(1)N-1 \,]$$

$$f_N(\underline{a}) = \frac{CA_e}{6} H \left[\frac{1}{A_o} + \frac{2}{A((N-3/2)H)} \right]$$

$$- \beta \frac{H}{6} \left[a_N (h - \frac{a_N^2}{2})^{5/2} + (a_{N-1} + a_N) (h - (\frac{a_{N-1} + a_N}{8})^2)^{5/2} \right] = 0 \qquad (3.7)$$

where β is a quantity defined in terms of the entropy by

$$\beta = \left[2/7\eta \right]^{5/2} . \qquad (3.8)$$

The system of equations is solved by Newton's method, where here the Jacobian matrix takes a particularly simple tri-diagonal form. Hence the linear system (2.57) is easily solved at each iteration level by L-U factorization.

3.2 NUMERICAL SOLUTION OF CONE SECTION FLOW

The particular domain on which a cone section lies is defined as

$$0.0 \leq x \leq 1.0 \ ; \tag{3.9}$$

the boundary nodal locations are therefore $S_1 = 0.0$ and $S_N = 1.0$, the interior nodes being equally spaced by a distance (1/N) apart.

A particular converging cone section flow is defined (see [4]) by the area variation

$$\begin{aligned} A(x) &= 1 + 0.1(1-x) + 0.05(1-x)^2 \ , \\ A_e &= 1.15 \ , \\ A_o &= 1.0 \ , \end{aligned} \tag{3.10}$$

as shown in FIG.3*i*, and prescription of the mass flow boundary conditions by

$$C = 200.0$$

and by (2.30)

$$Q_o = 230.0 \ . \tag{3.11}$$

By substitution of (3.10ab) and (3.11a) into (2.33) the associated unique stationary principle representative of this motion is

$$\delta \left[\int_D \left[\frac{230.0}{1 + 0.1(1-x) + 0.05(1-x)^2} v + p(v) \right] dx \right] = 0 \ . \quad (3.12)$$

A diverging section flow is also defined (see [4]), with the area variation illustrated in FIG.5i, by,

$$\begin{aligned} A(x) &= 1 + 0.1x + 0.05x^2 \ , \\ A_e &= 1.0 \ , \\ A_o &= 1.15 \ , \end{aligned} \quad (3.13)$$

$$\begin{aligned} C &= 230.0 \ , \\ Q_o &= 200.0 \ ; \end{aligned} \quad (3.14)$$

the corresponding stationary principle may be stated as

$$\delta \left[\int_D \left[\frac{230.0}{1 + 0.1x + 0.05x^2} v + p(v) \right] dx \right] = 0 \ . \quad (3.15)$$

Initial data regions

The flow throughout either of the cone section geometries may be subsonic or supersonic (see [4]), the definitive quantity being the critical fluid speed, C_*,

$$\begin{aligned} v < C_* &: \text{ SUBSONIC FLOW} \ , \\ v > C_* &: \text{ SUPERSONIC FLOW} \ , \end{aligned} \quad (3.16)$$

(see [1]). The critical value is that where the fluid speed equals the local sound speed and is dependent on the total energy within the flow (1.20a) and the adiabatic exponent associated with the fluid (1.19a), here we have

$$C_* = 302.5 \ ms^{-1} \ . \tag{3.17}$$

Hence there will exist, for a particular cone section, two independent solution vectors of the equation system (3.7), i.e. two fixed points, a^*, satisfying (2.51), corresponding to the two possible flow types defined by (3.16).

Correspondingly there are two positive distinct initial data regions. These depend on the number of nodes in the numerical formulation and in the present case are shown when employing five nodes in the numerical solution of both cone section motions

$$\begin{aligned} &[r1] \ : \ \underline{a}^{\circ} \in [1,287] \qquad \text{SUBSONIC FIXED POINT} \ , \\ &[r2] \ : \ \underline{a}^{\circ} \in [324,630] \qquad \text{SUPERSONIC FIXED POINT} \ . \end{aligned} \tag{3.18}$$

Specifying the constant initial data vector in one of these regions will result in convergence of the iterative method to the respective fixed point such that (2.51) is attained, subject to the tolerance (2.59). Assignment from [r1], say

$$\underline{a}^{\circ} = 200.0 \ , \tag{3.19}$$

will determine the piece-wise linear subsonic fluid speed variation for flow through both section geometries (see FIGS.3*ii*,5*ii*), and

alternatively from [r2], say

$$\underline{a}^{o} = 500.0 \ , \qquad (3.20)$$

the piece-wise linear supersonic fluid speed variation will be obtained (see FIGS.4*ii*,6*ii*).

The remaining flow variables associated with a cone section flow are related to the fluid speed by a set of algebraic relations, (see [3] and also the presentation in [4]), of which (2.40) is an example. Therefore if the subsonic and supersonic fluid speed variations throughout such a motion are considered as particular parameterizations of the flow in these relations then, for each, the piece-wise linear variation of all flow variables may be determined. The subsonic variation of all such flow variables through both cone section geometries is shown in FIGS.3,5 and the supersonic variation in FIGS.4,6.

In a similar manner by using a particular fluid speed variation as a set of intermediate numerical parameters in the algebraic relations a graphical representation of the approximate inter-variable relationship of any flow variable pair during the particular cone section motion may be obtained.

Relative error

An algebraic parameterisation for quasi one-dimensional duct flow is available in [4], through the derivation of a non-linear relationship between the fluid speed and the distance from inlet along the duct axis. The fluid speed variation throughout a motion is then obtained by the

specification of a range of axial locations between the duct inlet and outlet stations. The degree of accuracy to which this is computed allows the algebraic formulation to be used as an 'exact' solution to compare with the numerical results; results for the particular cone section motions considered here have already been calculated for both flow types in [4].

Therefore, for each of the section geometries, we now have two piece-wise linear functions representing the fluid speed variation throughout, which shall be denoted by f and g, each defined on a different grid but on the same domain [0,1]. A measure of the relative difference between them is possible by definition of a general relative L_2-norm, L_r, derived from

$$L_r^2 = \frac{\int_0^1 (f - g)^2 \, dr}{\int_0^1 \frac{(f + g)^2}{4} \, dr} \, . \qquad (3.21)$$

The relative error may be used, to test the accuracy of the numerical results, in particular in relation to the number of nodes used.

We specify arbitrarily that the numerical solution of a particular cone section motion is sufficiently accurate if the magnitude of the relative error satisfies:

$$\text{RELATIVE } L_2 \text{ ERROR} < 0.01 \, . \qquad (3.22)$$

The relative error for the numerical solution of both possible flow types through both cone section geometries, with various numbers of

nodes, is shown in TABLE.1.

CONVERGING AND DIVERGING CONE SECTIONS		
RELATIVE L2 ERROR BETWEEN NUMERICAL AND ALGEBRAIC SOLUTIONS		
NUMBER OF NODES	SUBSONIC FLOW	SUPERSONIC FLOW
5	0.0000645	0.0000279
7	0.0000283	0.0000122
9	0.0000158	0.0000068
11	0.0000101	0.0000043

TABLE.ONE

The fact that the relative error magnitude, in the numerical solution of the same flow type through both section geometries, is the same is a consequence of the fluid speeds being the inverse of each other.

All the values in TABLE.1 easily satisfy the accuracy condition (3.22). This would be expected from the qualitative appearance of the graphs of the algebraic parameterisations for these motions (see FIGS.3*viii*,4*viii*,5*viii*,6*viii* taken from [4]) which are nearly linear. The absence of curvature in these graphs allows the uniform fixed grid approach to represent the algebraic solution reasonably accurately.

On consideration of the accuracy condition (3.22) alone any of the number of nodes shown in TABLE.1 is sufficient in the numerical formulation, but by also taking into account computation time it is sensible to employ relatively few nodes, in the present case five.

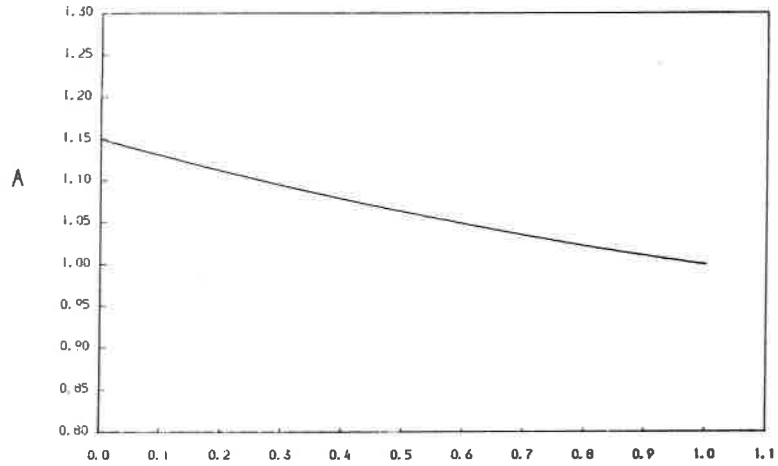

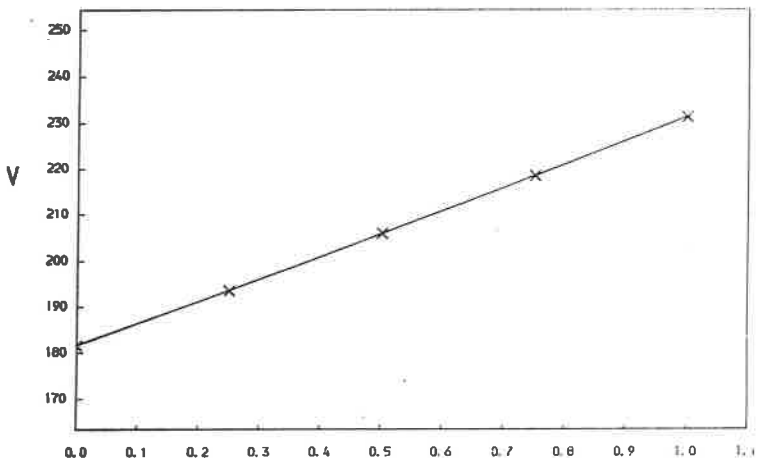

CONVERGING CONE SECTION : SUBSONIC FLOW

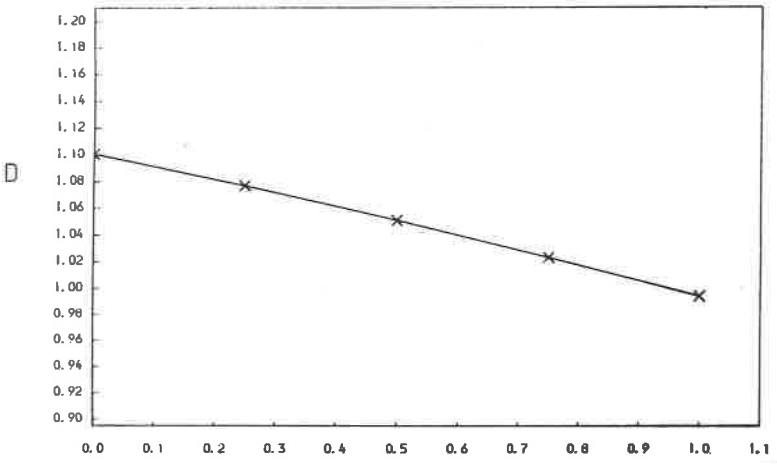

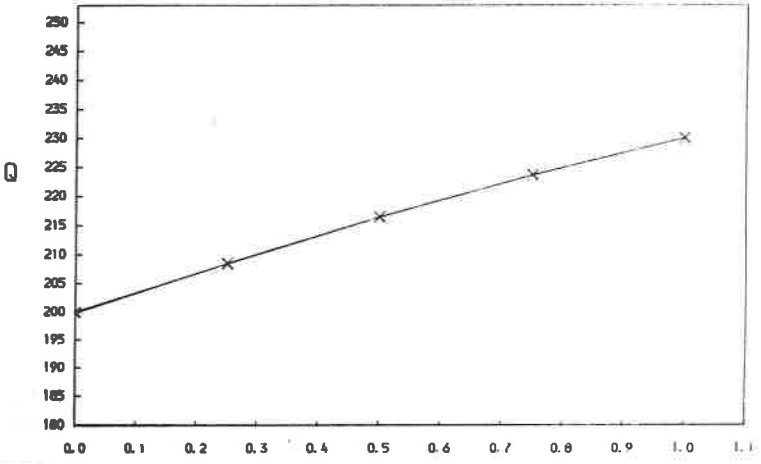

FIG THREE

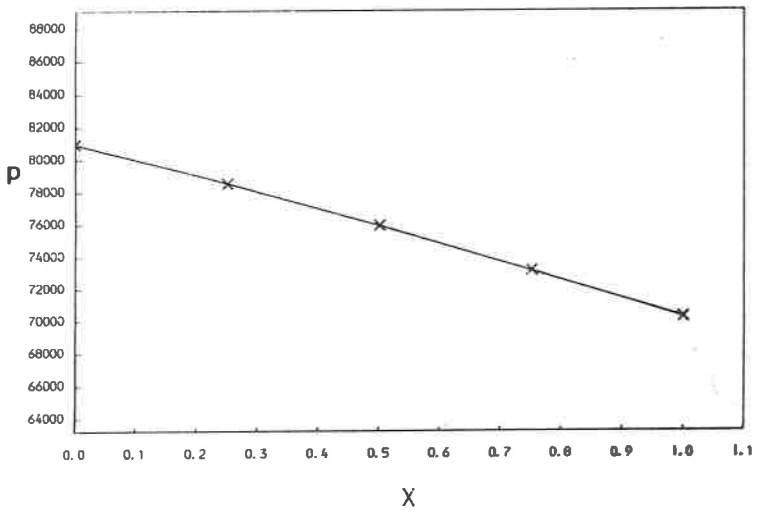

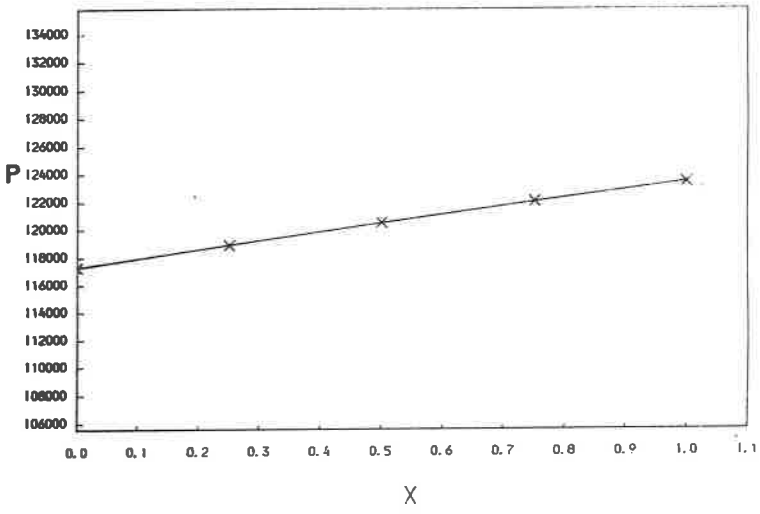

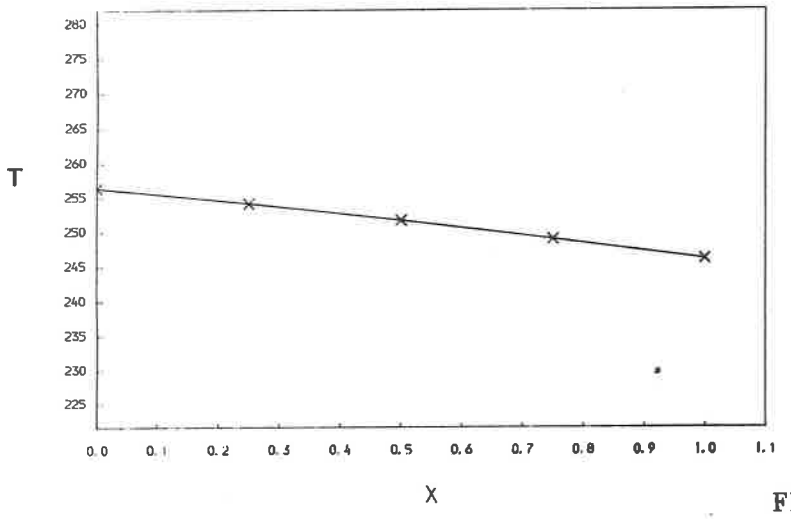

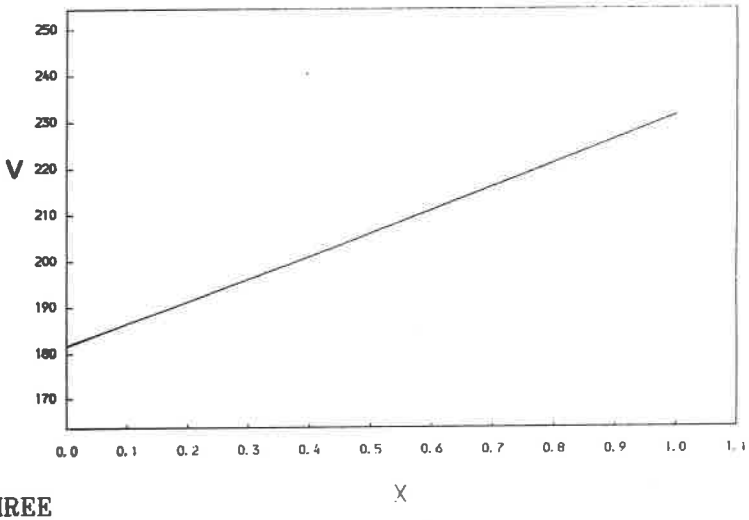

FIG THREE

cont.

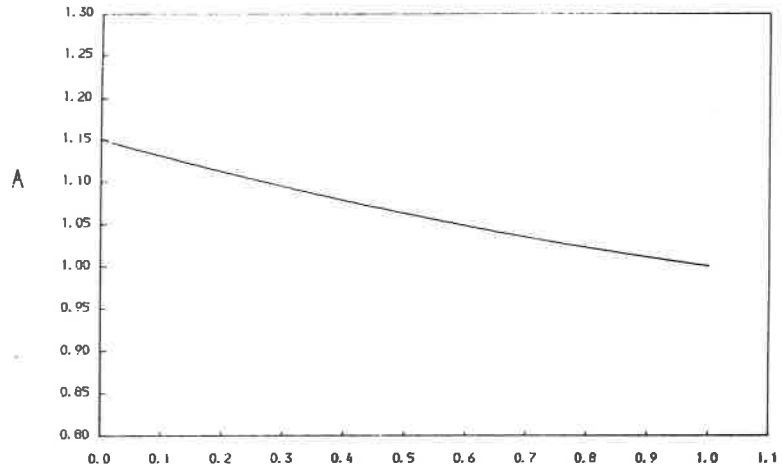

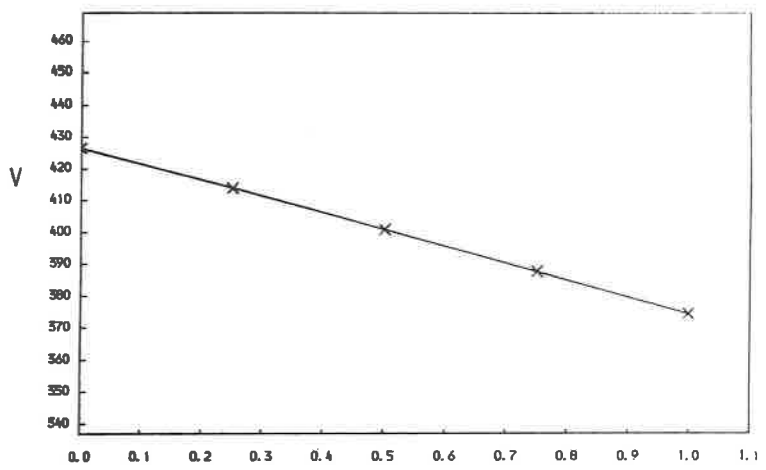

CONVERGING CONE SECTION : SUPERSONIC FLOW

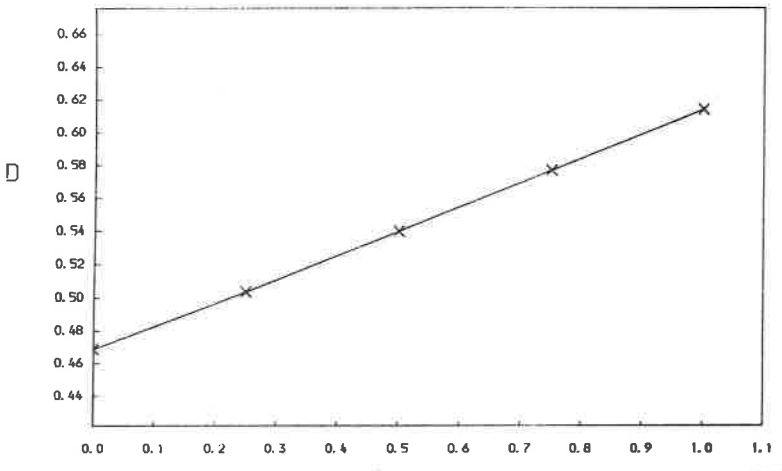

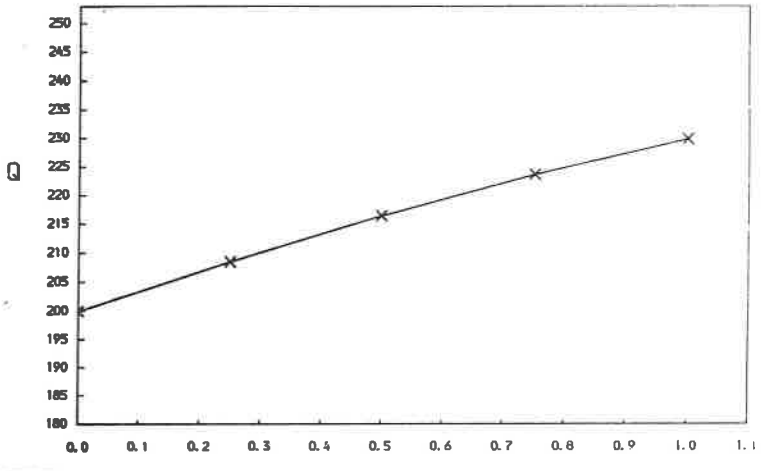

FIG FOUR

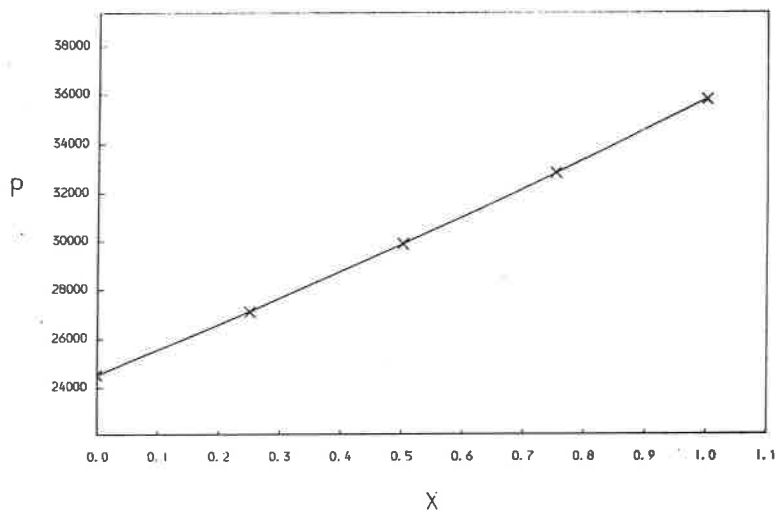

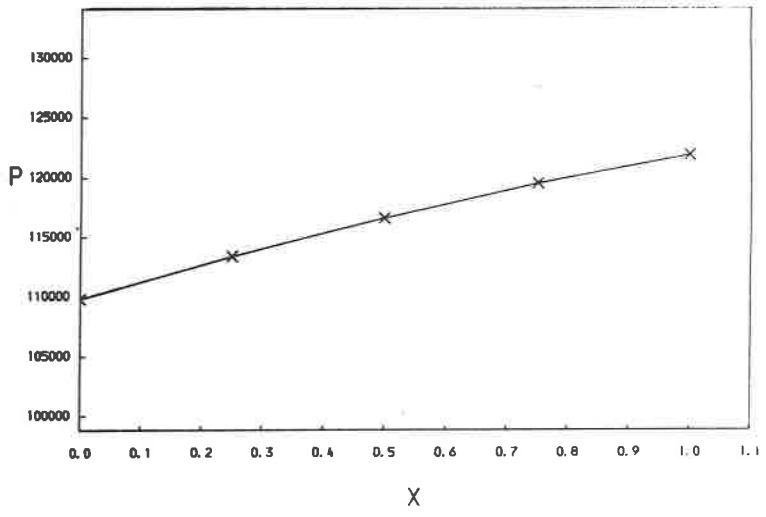

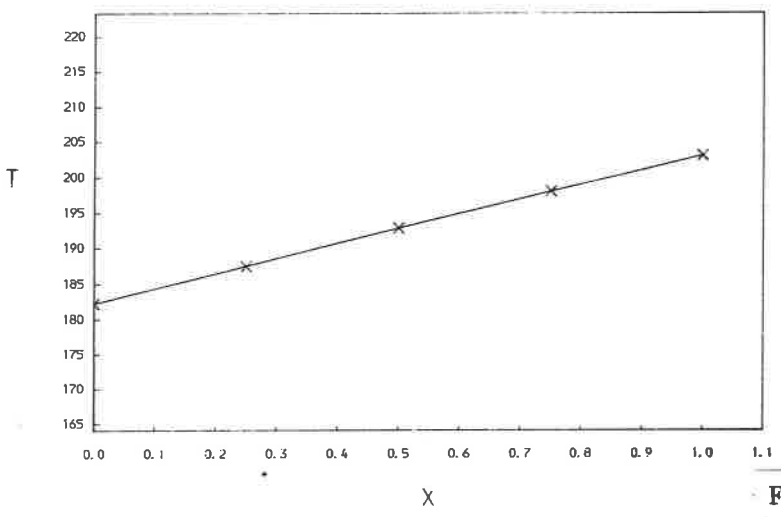

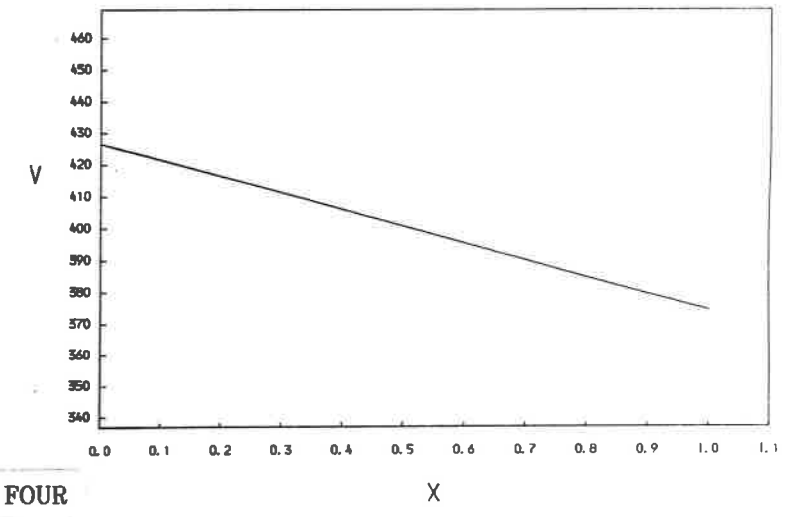

FIG FOUR

cont.

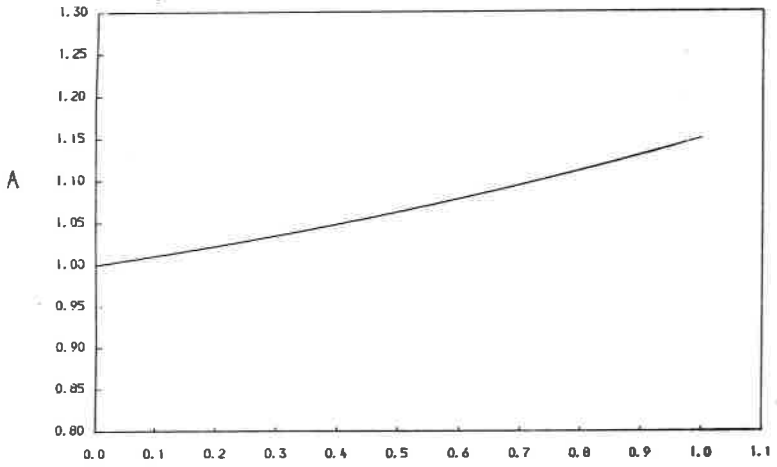

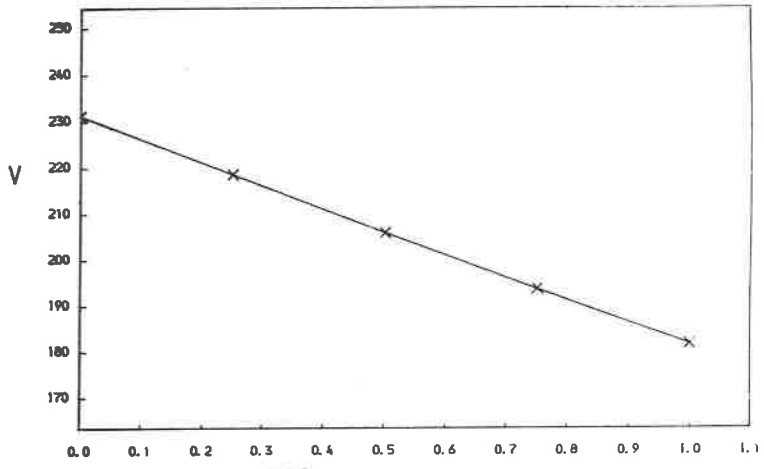

DIVERGING CONE SECTION : SUBSONIC FLOW

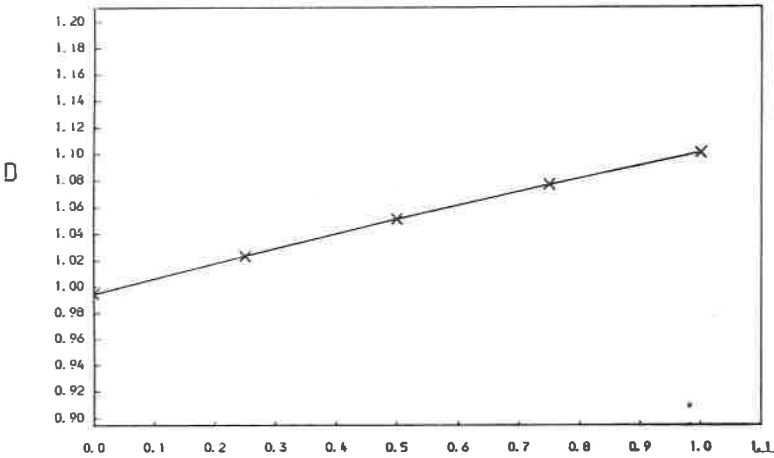

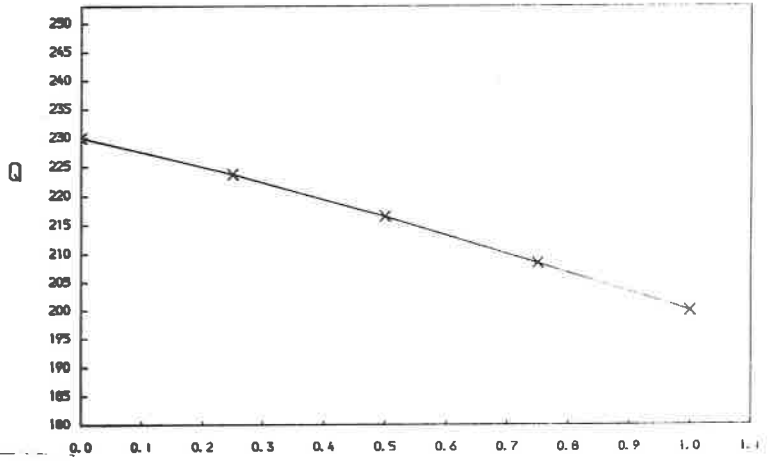

FIG.FIVE

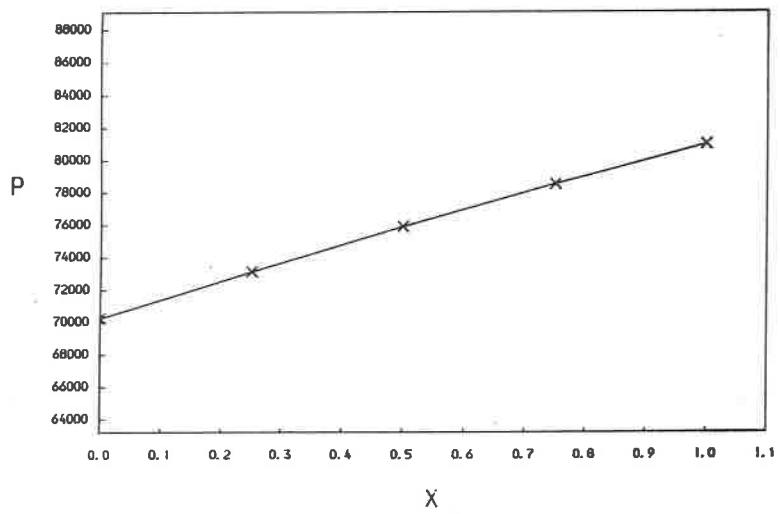

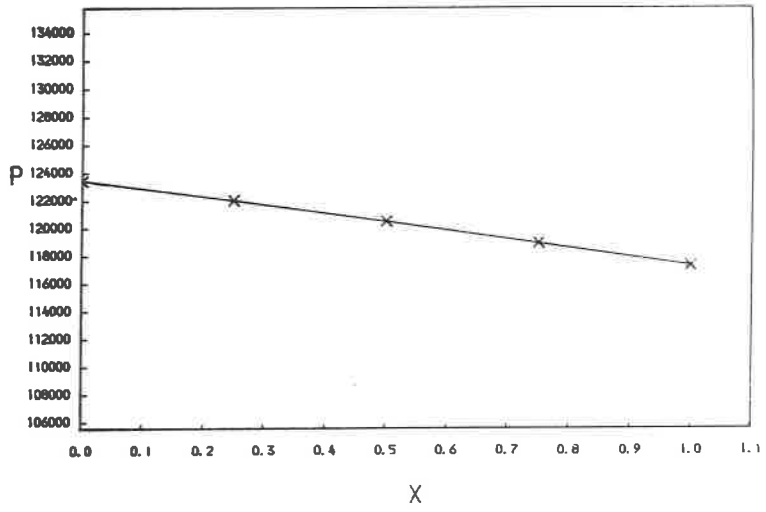

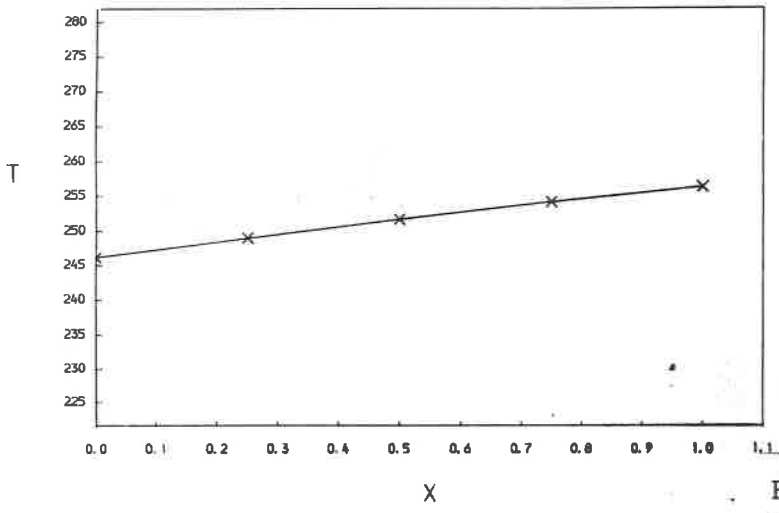

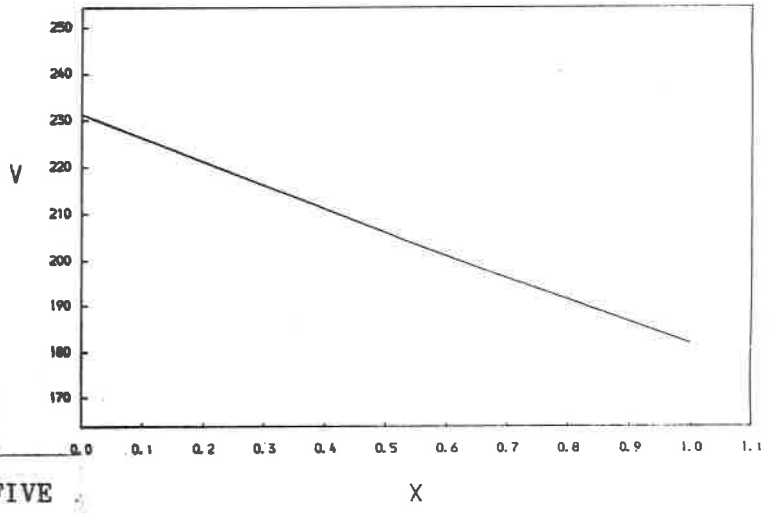

FIG FIVE

cont.

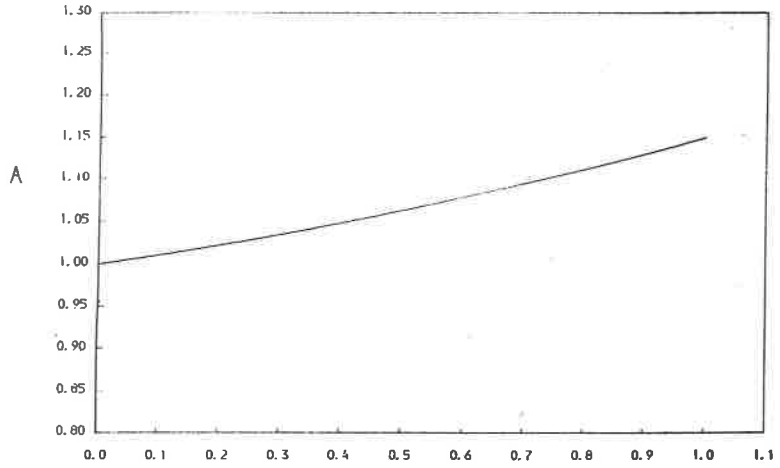

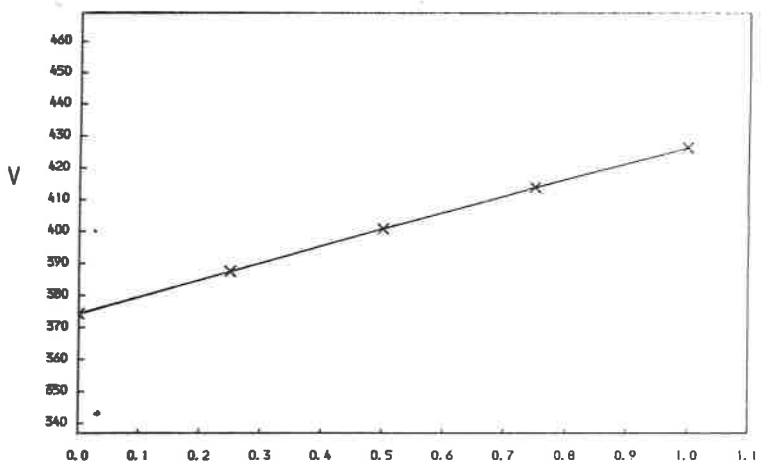

DIVERGING CONE SECTION : SUPERSONIC FLOW

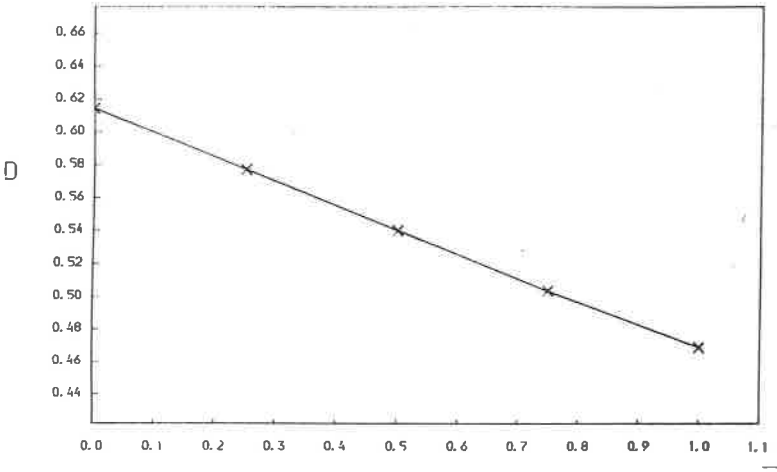

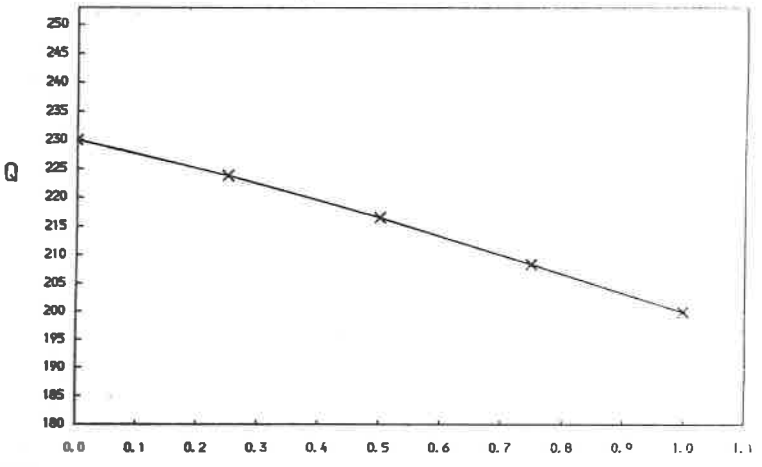

FIG-SIX

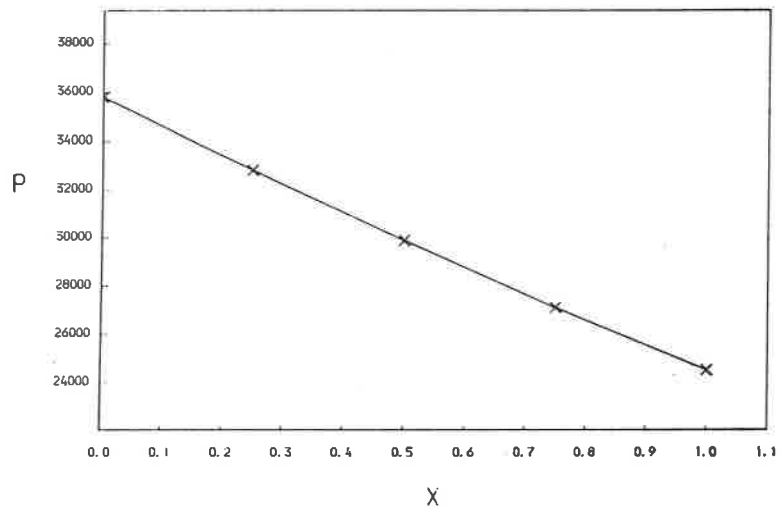
P
38000
36000
34000
32000
30000
28000
26000
24000
0.0 0.1 0.2 0.3 0.4 0.5 0.6 0.7 0.8 0.9 1.0 1.1
X

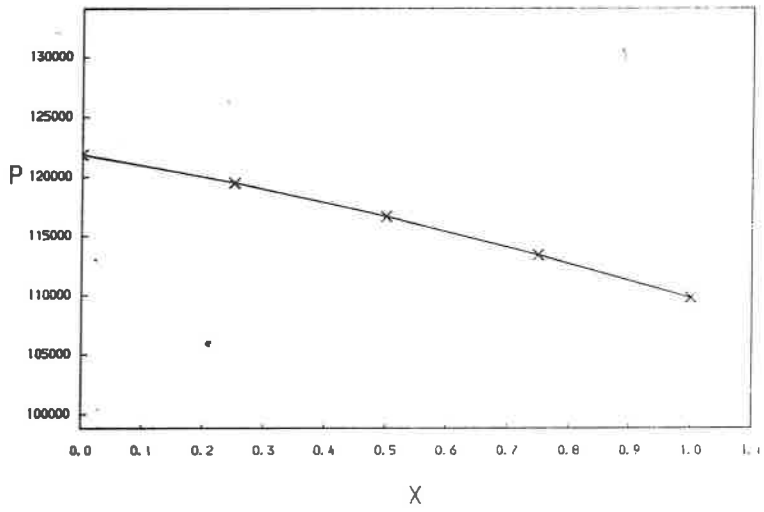
P
130000
125000
120000
115000
110000
105000
100000
0.0 0.1 0.2 0.3 0.4 0.5 0.6 0.7 0.8 0.9 1.0
X

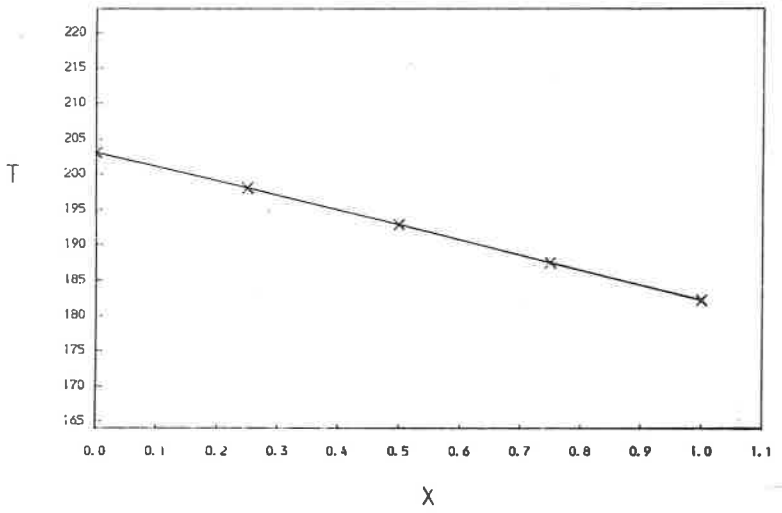
T
220
215
210
205
200
195
190
185
180
175
170
165
0.0 0.1 0.2 0.3 0.4 0.5 0.6 0.7 0.8 0.9 1.0 1.1
X

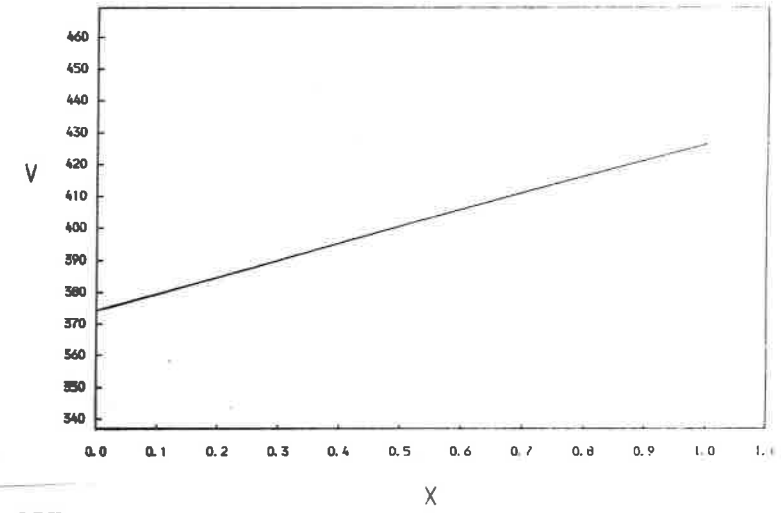
V
460
450
440
430
420
410
400
390
380
370
360
350
340
0.0 0.1 0.2 0.3 0.4 0.5 0.6 0.7 0.8 0.9 1.0
X

FIG SIX

cont.

3.3 NUMERICAL SOLUTION OF DE-LAVAL NOZZLE FLOW

The de-Laval nozzle is defined on the domain

$$0.0 \leq x \leq 2.0 \ , \tag{3.23}$$

by the area variation corresponding to the two composite sections

$$\begin{aligned} &\text{ENTRY SECTION} \quad : \quad A_1(x) = 1.1 - (x/8) && 0.0 \leq x \leq 0.8 \ , \\ &\text{EXHAUST SECTION} \quad : \quad A_2(x) = (2.6/3.0) + (x/6) && 0.8 \leq x \leq 2.0 \ , \end{aligned} \tag{3.24}$$

(see FIG.7*i*) with

$$\begin{aligned} A_e &= 1.1 \ , \\ A_T &= 1.0 \ , \\ A_o &= 1.2 \ , \end{aligned} \tag{3.25}$$

where A_T is the minimum cross-sectional area of the nozzle at the throat location, i.e. from (3.24) at x = 0.8. Boundary nodes are placed at $S_1 = 0.0$ and $S_N = 2.0$. The interior nodes are equally separated by a distance (2/N); the number of nodes is specified such that a node always lies at the nozzle throat location.

The entry mass flow rate to the central streamline is assigned by,

$$C = 223.9193 \ , \tag{3.26}$$

and the critical value of mass flow rate on that streamline, in this case is

$$Q_* = 246.31124 \ , \tag{3.27}$$

(see [4]) corresponding to the critical fluid speed (3.17) being attained at the throat. The outlet mass flow rate value is then, from (2.30)

$$Q_o = 205.25936 \ . \tag{3.28}$$

Te stationary principle representative of this motion given by (2.33) is,

$$\delta \left[\int_D \left[\frac{246.31124}{A(x)} v + p(v) \right] dx \right] = 0 \ , \tag{3.29}$$

where A(x) is defined by (3.24).

Initial data regions

The assumption is made that the flow enters the nozzle subsonically , therefore the mass flow rate at the throat being critical means that the flow in the exhaust section (diffuser) may take one of two forms. Dependant on the outlet pressure conditions it may remain subsonic throughout the nozzle, or a transition may occur at the throat and the flow will become supersonic in the diffuser (see [4]). It is in these two possible flow behaviours that interest lies.

There exist two independent solution vectors, satisfying (2.54), corresponding to subsonic flow, $\underline{a}^*_{sub}$, and supersonic flow, $\underline{a}^*_{sup}$, throughout the complete nozzle and, as in cone section flow, two initial data regions. The exact bounds of the initial data regions again depends on the number of nodes in the numerical formulation and are shown in the present case for when employing twenty-one nodes

$$\begin{aligned} &[R1] \;:\; \underline{a}^\circ \in [1,287] \qquad \text{SUBSONIC FIXED POINT} , \\ &[R2] \;:\; \underline{a}^\circ \in [322,625] \qquad \text{SUPERSONIC FIXED POINT} . \end{aligned} \tag{3.30}$$

Prescription of the constant initial data vector in each of these regions causes convergence of the iterative solution method to the respective fixed point. Particular to de-Laval nozzle flow there also exists a third fixed point as a linear combination of the two already stated. This corresponds to the possibility of transition flow explained above and will therefore be denoted by a^*_{trans}.

The piece-wise linear approximation to the subsonic fluid speed variation throughout the nozzle is obtained by specifying the constant initial data vector,

$$\underline{a}^\circ = 200.0 , \tag{3.31}$$

(see FIG.7*ii*). The determination of the approximation to transition flow is by a process analagous to the analytic fixed point theory. The piece-wise linear approximation to supersonic flow throughout the nozzle is first computed by prescribing the constant initial data vector

$$\underline{a}^{o} = 500.0 \ , \tag{3.32}$$

and a linear combination, about the throat node, is then taken between this solution vector and that obtained for the subsonic flow. This is performed in the following manner

$$a^{*}_{trans} = \begin{cases} a^{*}_{sub} : & a^{*}_{1_{sub}} \leq a^{*}_{i_{sub}} \leq a^{*}_{T_{sub}} \\ a^{*}_{sup} : & a^{*}_{T_{sup}} < a^{*}_{i_{sup}} \leq a^{*}_{N_{sup}} \ . \end{cases} \tag{3.33}$$

where $a^{*}_{T_{sub}}$ and $a^{*}_{T_{sup}}$ are nodal numerical solutions at the throat (see FIG.8*ii*). Note that it would seem viable to obtain the transition flow approximation in a more fundamental manner by specifying the initial data vector as a linear combination, about the throat node, of (3.31) and (3.32), i.e.

$$\begin{aligned} \underline{a}^{o} &= 200.0 \qquad a^{o}_{1} \leq a^{o}_{i} \leq a^{o}_{T} \ , \\ \underline{a}^{o} &= 500.0 \qquad a^{o}_{T} < a^{o}_{i} \leq a^{o}_{N} \ , \end{aligned} \tag{3.34}$$

but this produces large gradients in the initial data around the nozzle throat. Consequently in that region of the solution domain there occurs, whatever the choice of initial data value for the node at the throat, unacceptable oscillations in the final converged solution vector.

Using the two fluid speed solution vectors, associated with the two flow behaviours of interest in the nozzle, as particular parameterizations of the flow in the algebraic relations (see §3.2), the

variation of all of the flow variables in the flow may be determined (see FIGS.7,8). Graphs of the relationship between any flow variable pair during a motion may also be simply derived.

Relative error

A comparative 'exact' solution for the particular de-Laval nozzle motion considered here is available from [4]. Therefore the relative difference between the numerical solution and this formulation may be computed using (3.21). The critical point being attained at the throat means that, for the numerical solution of both flow behaviours, the converged solution value at the throat node may be overwritten by the critical fluid speed value (3.17), i.e.

$$a_T^* = 302.5 \ . \qquad (3.35)$$

The magnitude of the relative error for a range of numbers of nodes used in the numerical formulation, for both flow behaviours, is shown in TABLE.2.

DE-LAVAL NOZZLE		
RELATIVE ERROR BETWEEN NUMERICAL AND ALGEBRAIC SOLUTIONS		
NUMBER OF NODES	SUBSONIC FLOW	TRANSITION FLOW
11	0.0158	0.0095
15	0.0105	0.0063
21	0.0078	0.00465

TABLE.TWO

The significant decrease in accuracy of these solutions, compared to those obtained for the cone section motions (see TABLE.1), is due to the relatively large curvature, i.e. rate of fluid speed change, present around the nozzle throat. This can be clearly seen from the algebraic formulations of these flows (see FIGS.7*viii*,8*viii* from [4]). The relative accuracy condition (3.22) can only be met by employing twenty-one nodes in the numerical formulation of subsonic flow, which is computationally expensive (note that the same number is used in the approximation to transition flow for consistency). It can therefore be concluded that the present numerical approach is not very efficient when significant curvature occurs in the solution.

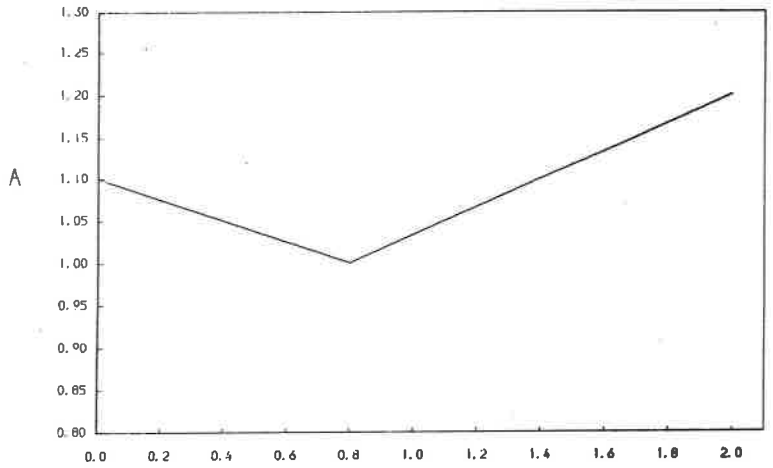

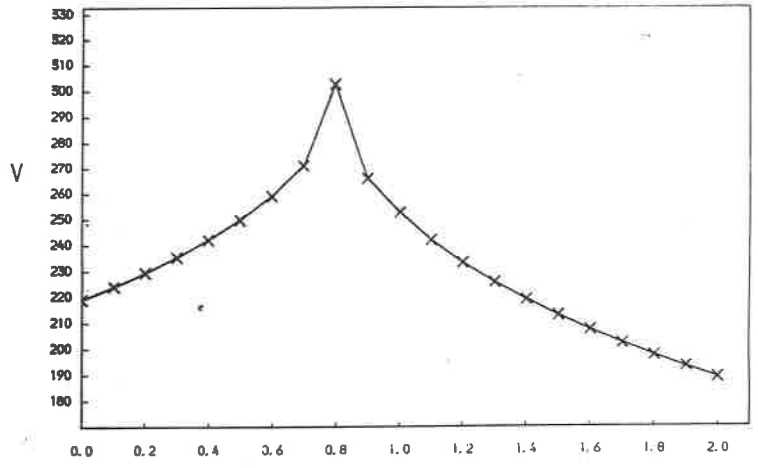

DE-LAVAL NOZZLE : SUBSONIC FLOW

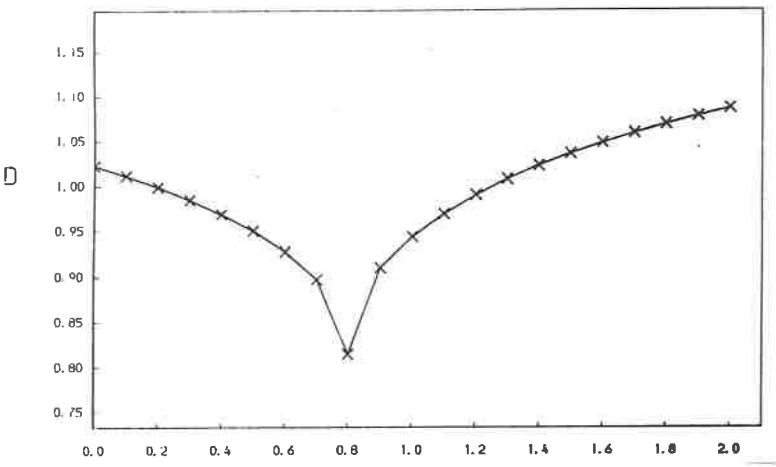

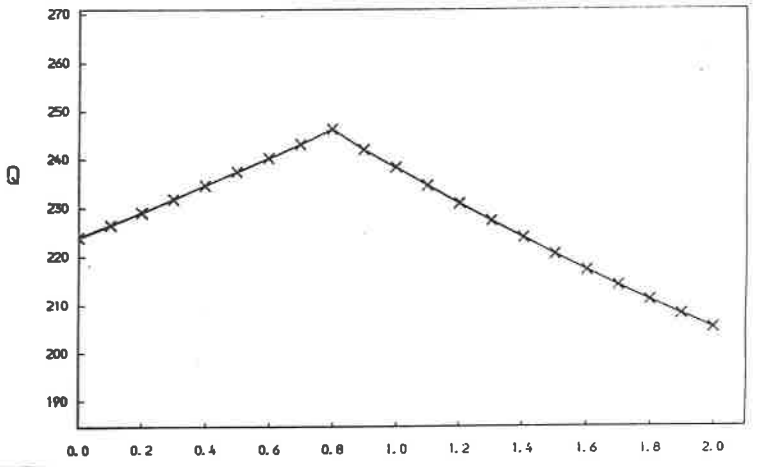

FIG SEVEN

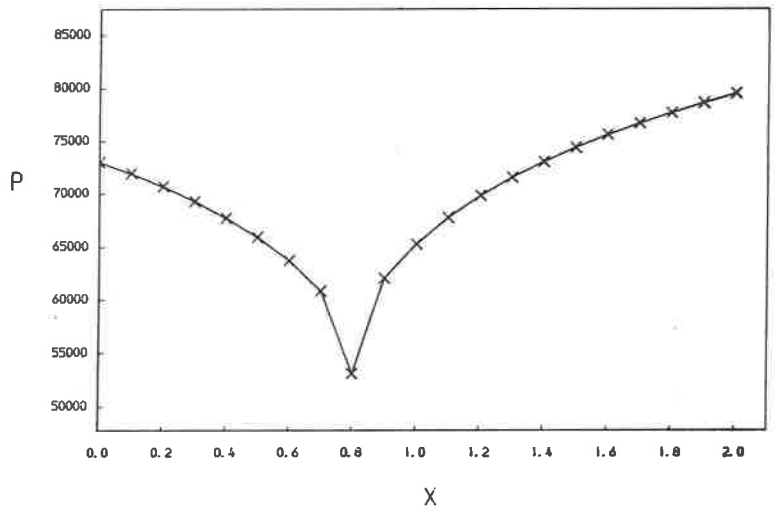

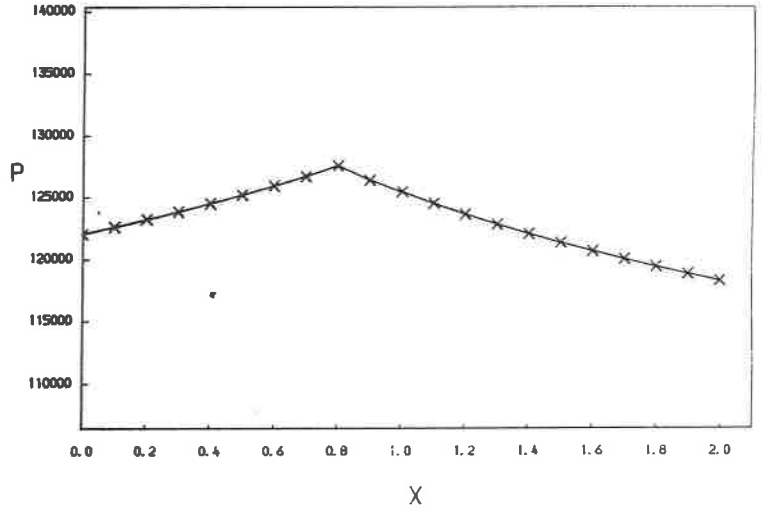

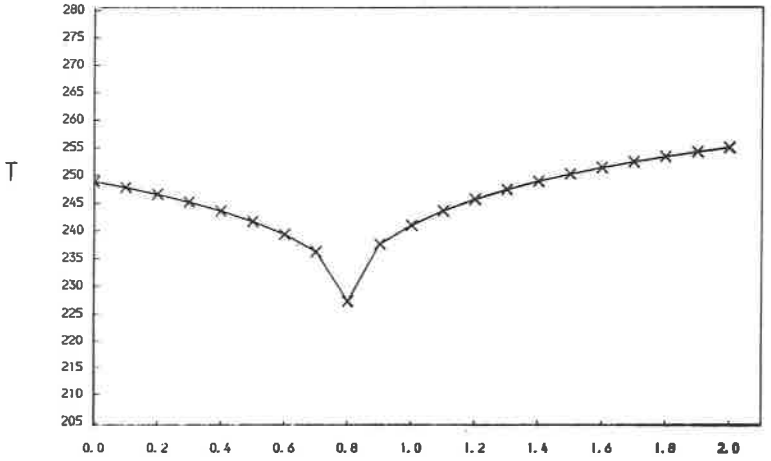

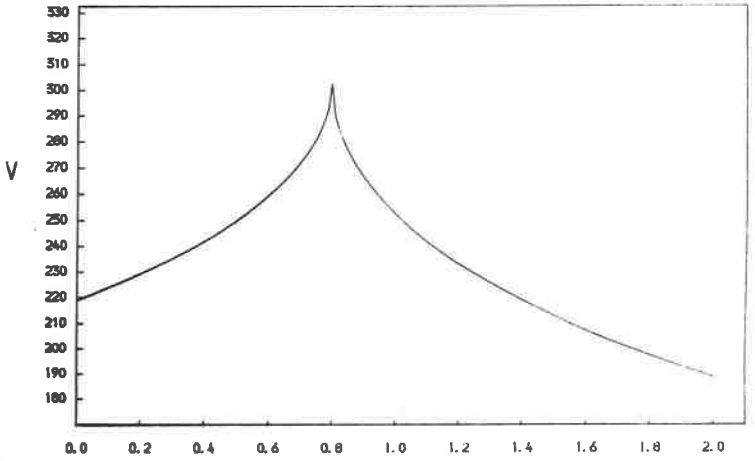

FIG SEVEN

cont.

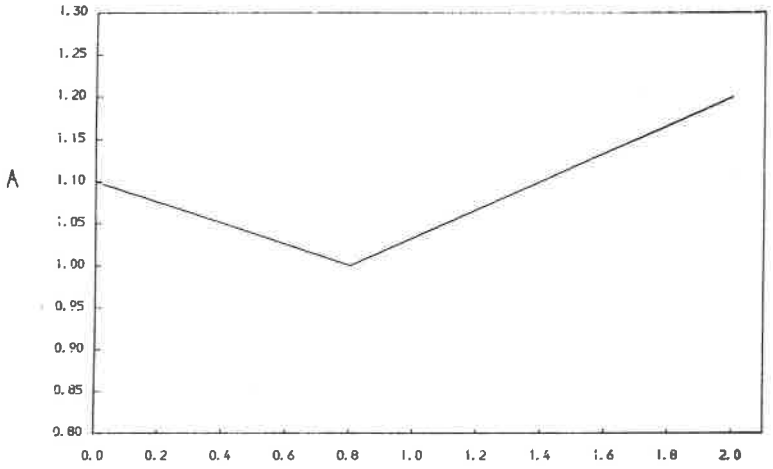

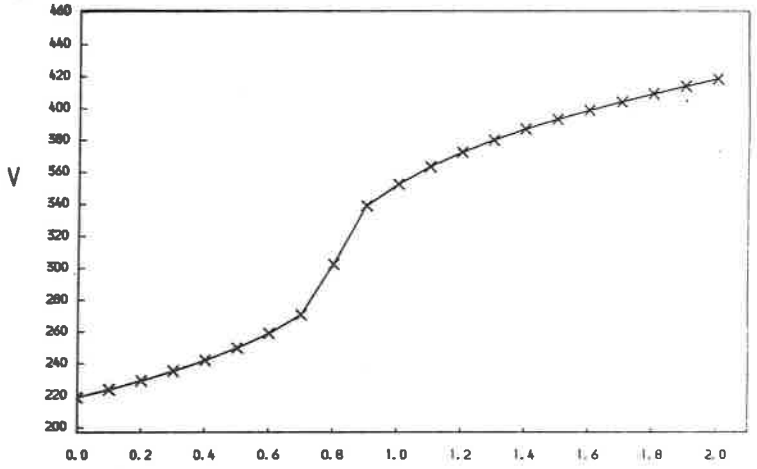

DE-LAVAL NOZZLE : TRANSITION FLOW

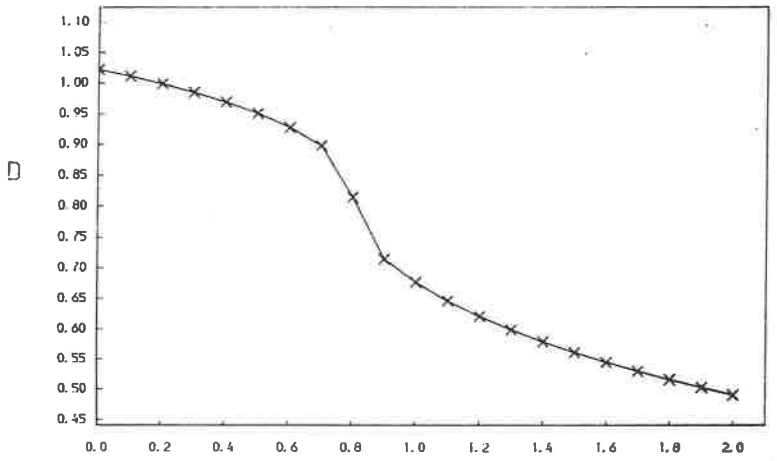

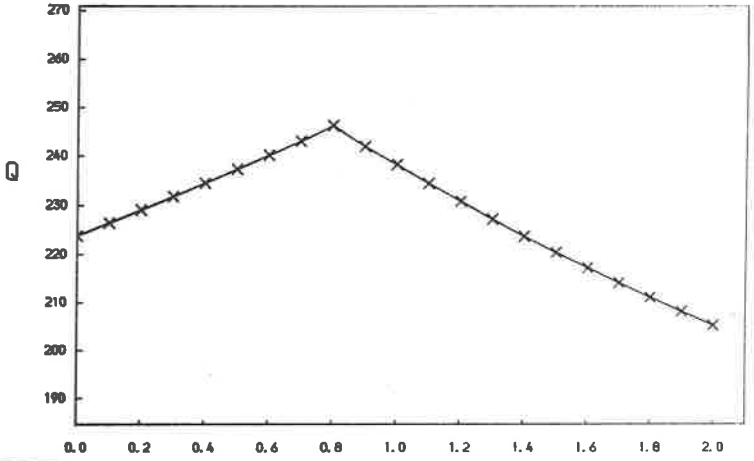

FIG EIGHT

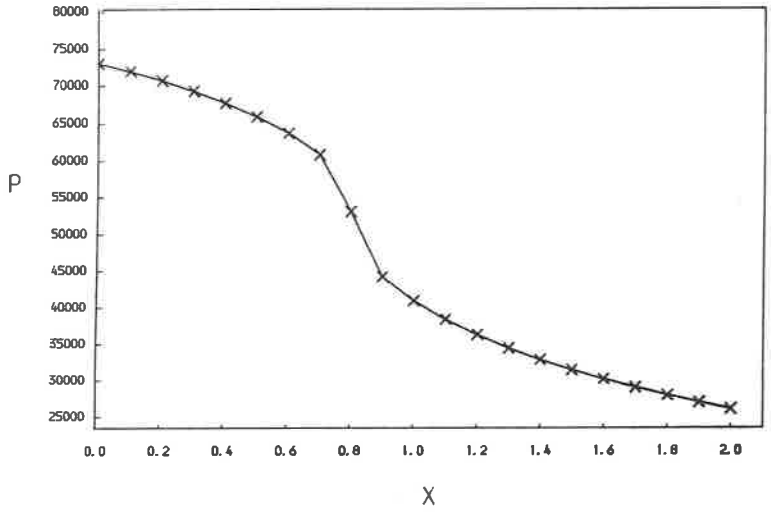

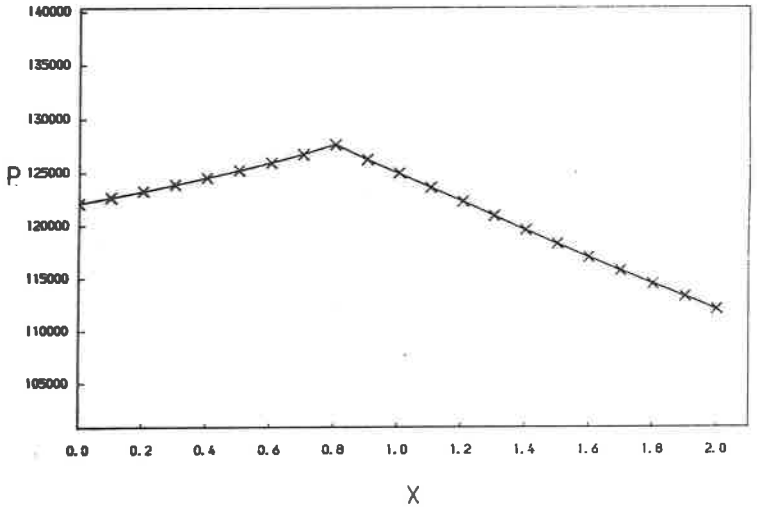

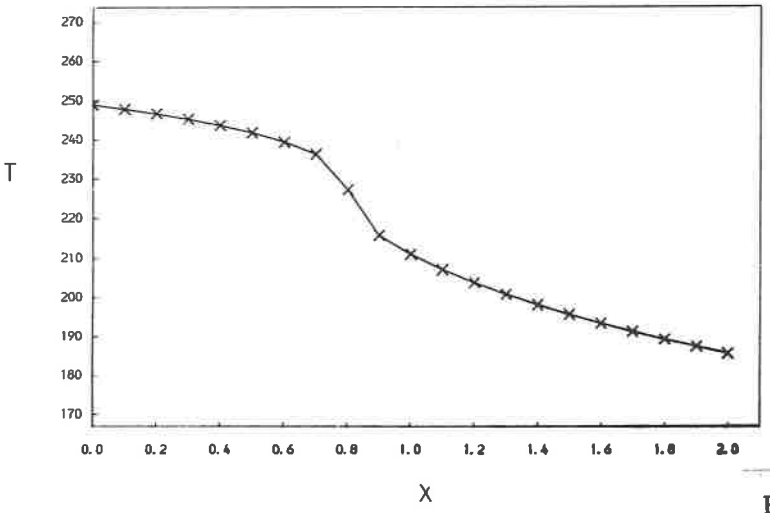

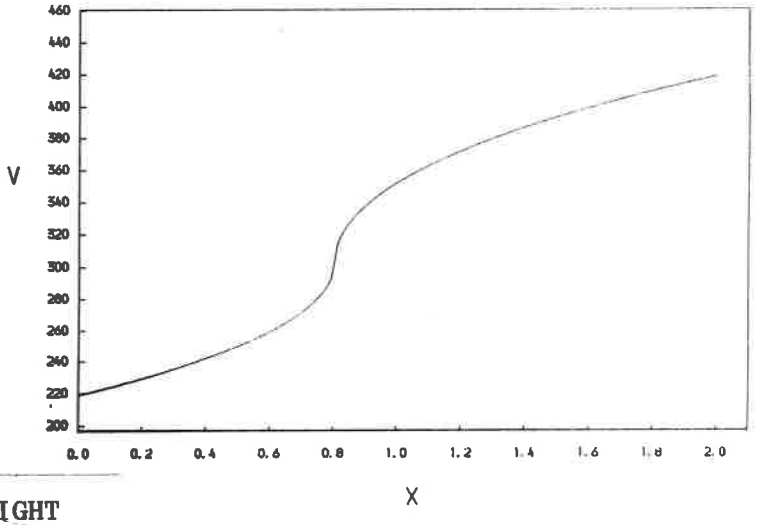

FIG EIGHT

cont.

SECTION FOUR : IMPLEMENTATION OF THE NUMERICAL METHOD ON AN IRREGULAR GRID

It is apparent from the results obtained for the numerical solution of cone section flow and de-Laval nozzle flow on a uniform grid (see §3) that the definition of the grid itself plays a critical role in the consideration of the applicability of a numerical method to the solution of a particular problem.

The curvature present in the solution of the de-Laval nozzle flow (§3.3) suggests a re-definition of the present uniform grid is needed if a solution of the same order of accuracy as that for cone section flow is to be achieved inexpensively. One possible approach is to use a fixed irregular grid. The number of nodes in the formulation remains the same but these are now re-distributed throughout the solution domain, using a-priori knowledge of the actual solution, so as to improve the representation of known solution features and hence improve the relative accuracy of the numerical solution. Alternatively if the key issue is computational effort then the same order of accuracy may be achieved on an irregular grid as on a uniform grid, with fewer nodes employed.

Knowledge of the solution has been assumed here although this is usually not available. The following results do though give useful insight into the benefits of grid re-definition and also provide a link to adaptive grid techniques which will be presented in the next report.

The particular nozzle motion to be considered is defined by (3.24)-(3.28) and lies on the domain (3.23). The exact solution of this motion is available from [4] and graphs of the parameterizations of both subsonic and transition flow are shown in FIGS.7*viii*,8*viii*.

4.1 GRID DEFINITION

The irregular grid is specified such that the boundary nodal positions lie at the domain extremes,

$$S_1 = 0.0$$

and (4.1)

$$S_N = 2.0 \ .$$

The interior nodal positions are then determined in two stages.

1. Polynomial interpolation of algebraic formulation

Flow through the nozzle is considered to occur in two distinct stages, the division being at the nozzle throat. An exact interpolation polynomial, p, of degree n is then passed through n+1 selected points (x_i, y_i), i = 0(1)n, calculated by the method used in [4], in each stage of the flow. Thus two such polynomials will represent a full nozzle flow, each of which is unique over its respective domain, such that

$$p(x_i) = y_i \ , \qquad i = 0(1)n$$

where (4.2)

$$p(x_i) = \bar{a}_0 + \bar{a}_1 x_i + \bar{a}_2 x_i^2 + \ldots + \bar{a}_n x_i^n \ ,$$

and $\bar{a}_i$, i = 0(1)n, are the unknown polynomial coefficients. The coefficients in each polynomial are obtained by writing the associated n+1 equations of the form (4.2a) as a linear system

$$\begin{bmatrix} 1 & x_0 & x_0^2 & x_0^3 & \cdots\cdots & x_0^n \\ 1 & x_1 & x_1^2 & x_1^3 & \cdots\cdots & x_1^n \\ \vdots & & & & & \vdots \\ 1 & x_n & x_n^2 & x_n^3 & \cdots\cdots & x_n^n \end{bmatrix} \begin{bmatrix} \bar{a}_0 \\ \bar{a}_1 \\ \vdots \\ \bar{a}_n \end{bmatrix} = \begin{bmatrix} y_0 \\ y_1 \\ \vdots \\ y_n \end{bmatrix}, \quad (4.3)$$

where the coefficient matrix is Vandermonde, and solving with an efficient Gauss elimination routine.

2. Equi-distribution of nodes (see [8])

The specified number of nodes to be used in the numerical formulation in each nozzle section, are then equi-distributed over the respective interpolating polynomial with respect to the square root of its second derivative. This process uses fixed nodes at the ends of the domain on which the polynomial is defined and distributes the remainder internally dependent on the curvature. Thus we produce a numerical grid for the solution of a full nozzle flow, where a node will again appear at the nozzle throat location.

The computed numerical grids, when employing twenty-one nodes, for application to the solution of both subsonic and transition flow are given in TABLE.3 ; the grid used for subsonic flow is also illustrated in FIG.9. For both grids the number of nodes in each section of the nozzle is the same as was present on the uniform grid; a node is also, as stated, at the throat location. Both of the computed numerical grids, corresponding to the two possible flow behaviours, will be identical up to the throat position due to the assumption that the flow always enters the nozzle subsonically.

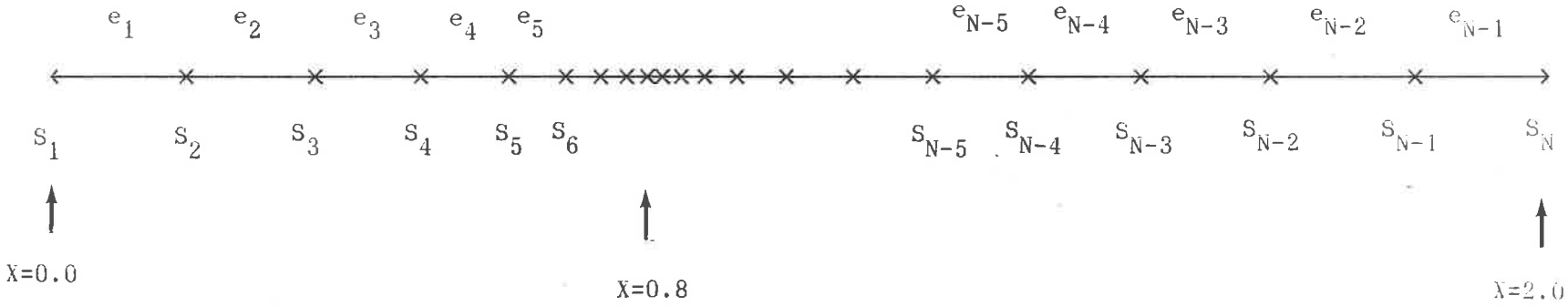
e1
e2
e3
e4
e5
eN-5
eN-4
eN-3
eN-2
eN-1
S1
S2
S3
S4
S5
S6
SN-5
SN-4
SN-3
SN-2
SN-1
SN
X=0.0
X=0.8
X=2.0

FIG NINE

NUMERICAL GRID FOR NOZZLE FLOW WITH TWENTY-ONE NODES					
NODE #	SUB'	TRANS	NODE #	SUB'	TRANS'
1	0.0	0.0	11	0.845	0.845
2	0.182	0.182	12	0.876	0.877
3	0.354	0.354	13	0.919	0.920
4	0.496	0.496	14	0.985	0.986
5	0.614	0.614	15	1.074	1.075
6	0.690	0.690	16	1.180	1.181
7	0.737	0.737	17	1.308	1.308
8	0.772	0.772	18	1.457	1.456
9	0.8	0.8	19	1.629	1.627
10	0.820	0.821	20	1.822	1.820
			21	2.0	2.0

TABLE.THREE

4.2 FORMULATION

The stationary principle corresponding to the motion is again (3.29), although the discrete function (2.36) will now differ numerically due to the non-uniformity of the basis functions. These are thus best defined here in the general manner (2.43).

Making this function stationary will again result in a system of equations. On application of the same numerical quadrature (2.46) a system of non-linear equations for the unknown nodal amplitudes, rather more complex than (3.7), is produced,

in which

$$f_1(\underline{a}) = \frac{CA_e}{6} E_1 \left[\frac{1}{A_e} + \frac{2}{A(E_1/2)} \right]$$

$$- \frac{\beta}{6} E_1 \left[a_1 (h - \frac{a_1^2}{2})^{5/2} + (a_1 + a_2) (h - (\frac{a_1 + a_2}{8})^2)^{5/2} \right] = 0$$

$$f_i(\underline{a}) = \frac{CA_e}{6} E_{i-1} \left[\frac{1}{A(S_i)} + \frac{2}{A(S_i - (E_{i-1}/2))} \right]$$

$$+ \frac{CA_e}{6} E_i \left[\frac{1}{A(S_i)} + \frac{2}{A(S_i + (E_i/2))} \right]$$

$$- \frac{\beta}{6} E_{i-1} \left[a_i (h - \frac{a_i^2}{2})^{5/2} + (a_{i-1} + a_i) (h - (\frac{a_{i-1} + a_i}{8})^2)^{5/2} \right]$$

$$- \frac{\beta}{6} E_i \left[a_i (h - \frac{a_i^2}{2})^{5/2} + (a_{i+1} + a_i) (h - (\frac{a_{i+1} + a_i}{8})^2)^{5/2} \right] = 0$$

$$[\ i = 2(1)N-1\ ]$$

$$f_N(\underline{a}) = \frac{CA_e}{6} E_{N-1} \left[\frac{1}{A_o} + \frac{2}{A(2 - (E_{N-2}/2))} \right]$$

$$- \frac{\beta}{6} E_{N-1} \left[a_N (h - \frac{a_N^2}{2})^{5/2} + (a_{N-1} + a_N) (h - (\frac{a_{N-1} + a_N}{8})^2)^{5/2} \right] = 0$$

(4.4)

, in terms of the nodal positions and associated element lengths

$$E_i = S_{i+1} - S_i \ , \qquad (4.5)$$

where

$$\beta = \left[2/7\eta \right]^{5/2}. \qquad (4.6)$$

This system is again solved by Newton's method. The initial data is assigned in accordance with the convergence regions (3.31) derived previously for twenty-one nodes in the formulation.

Therefore the piece-wise linear approximation to subsonic flow on the irregular grid (FIG.10*ii*) is obtained by specifying the constant initial data (3.31). The approximation to transition flow (FIG.11*ii*) is found by firstly deriving the supersonic solution vector (by specifying (3.32)) and then, as before, by taking a linear combination of this with the subsonic solution vector about the throat node (see (3.33)).

The variation of all of the remaining flow variables throughout the types of flow is subsequently computed (FIGS.10,11). The graphs of the relations between any flow variable pair throughout the flows may also be derived.

Relative error

The relative error in the numerical solution of both subsonic and transition flow is computed using (3.21), not only for the twenty-one nodes that were used in the uniform grid, but in addition for the same problem solved on an irregular grid of eleven nodes (see TABLE.4).

DE-LAVAL NOZZLE		
RELATIVE L2 ERROR BETWEEN NUMERICAL AND ALGEBRAIC SOLUTIONS		
NUMBER OF NODES	SUBSONIC FLOW	TRANSITION FLOW
11	0.00408	0.00279
21	0.00144	0.00099

TABLE.FOUR

Comparison of TABLE.4 with TABLE.2 shows the significant increase in relative accuracy obtained by the numerical solution of the present motion, for the same number of nodes, on the irregular grid used in preference to a uniform grid. The actual percentage decrease in magnitude of the relative error is found in TABLE.5.

DE-LAVAL NOZZLE		
PERCENTAGE DECREASE IN RELATIVE L2 ERROR		
NUMBER OF NODES	SUBSONIC FLOW	TRANSITION FLOW
11	74.22	70.1
21	81.5	78.9

TABLE.FIVE

The accuracy condition (3.22) is now met with eleven nodes in the formulation and we see that this solution is, for both types of flow, more accurate in terms of the norm considered than was the case for twenty-one nodes on the uniform grid. This is a consequence of the superior representation of the curvatures of the fluid speed near the nozzle throat.

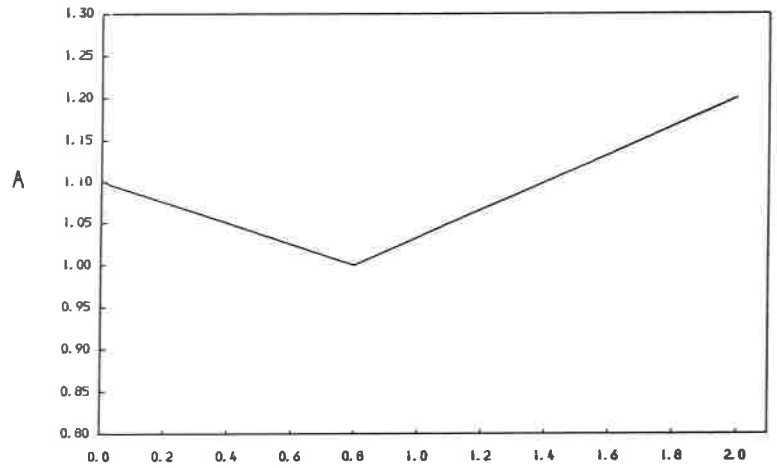

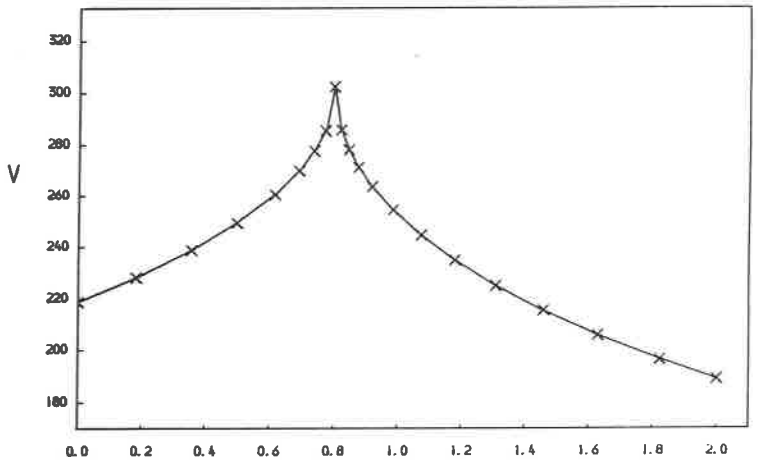

DE-LAVAL NOZZLE : SUBSONIC FLOW

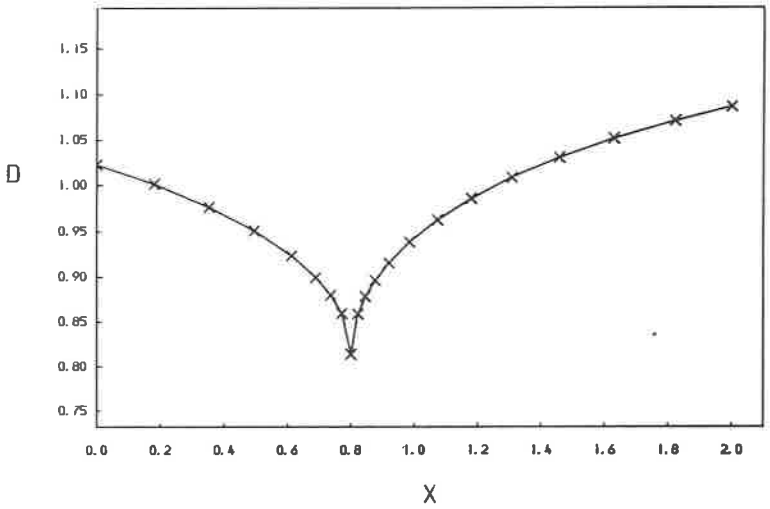

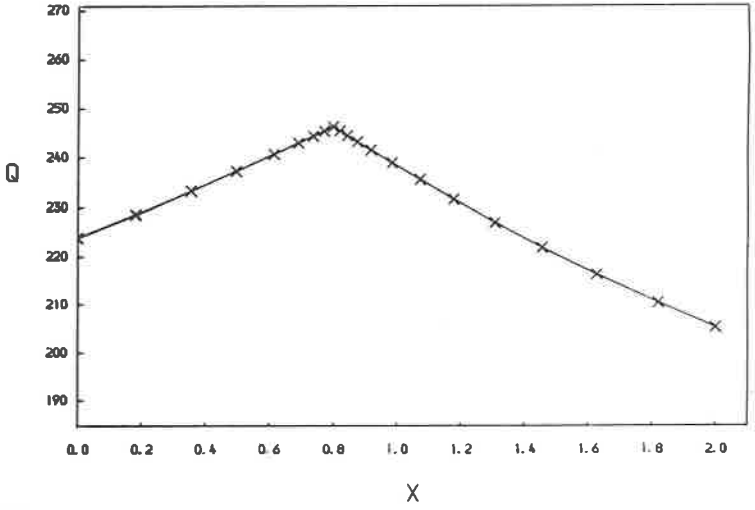

FIG TEN

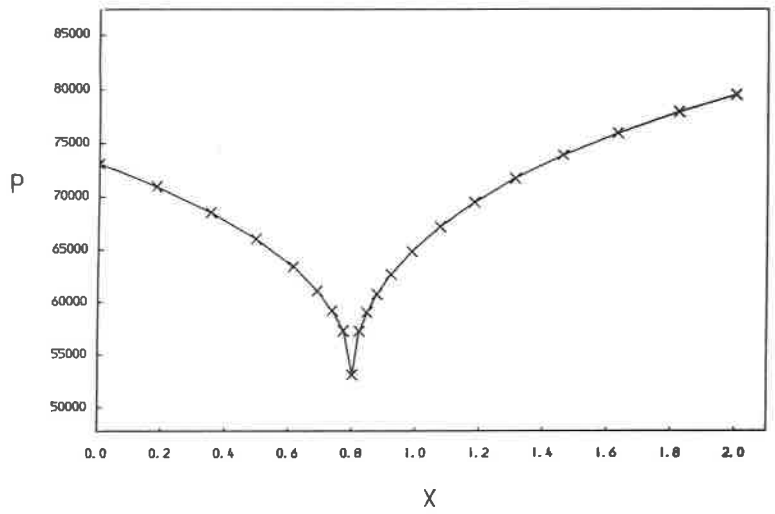
P
85000
80000
75000
70000
65000
60000
55000
50000
0.0 0.2 0.4 0.6 0.8 1.0 1.2 1.4 1.6 1.8 2.0
X

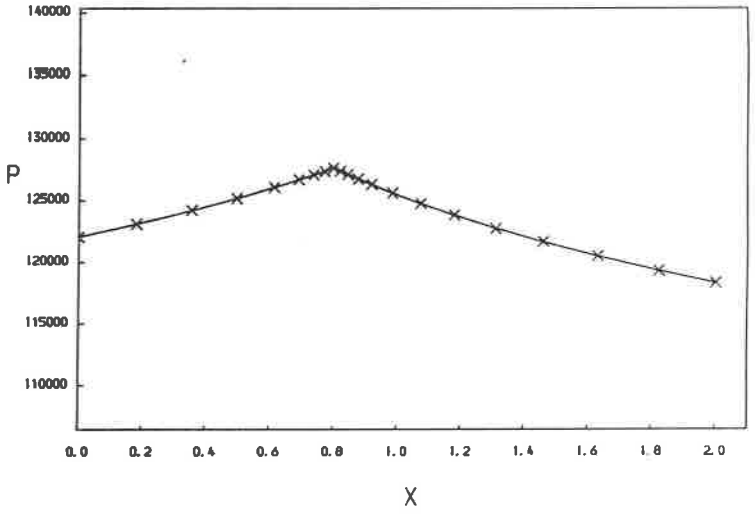
P
140000
135000
130000
125000
120000
115000
110000
0.0 0.2 0.4 0.6 0.8 1.0 1.2 1.4 1.6 1.8 2.0
X

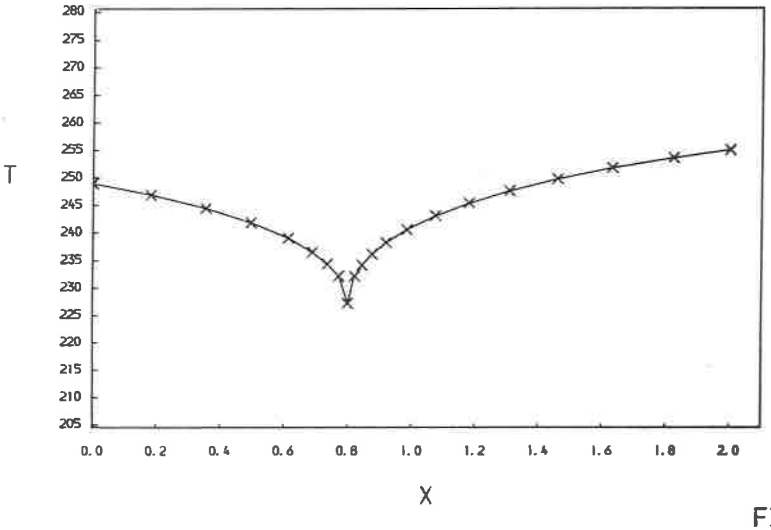
T
280
275
270
265
260
255
250
245
240
235
230
225
220
215
210
205
0.0 0.2 0.4 0.6 0.8 1.0 1.2 1.4 1.6 1.8 2.0
X

FIG TEN

cont.

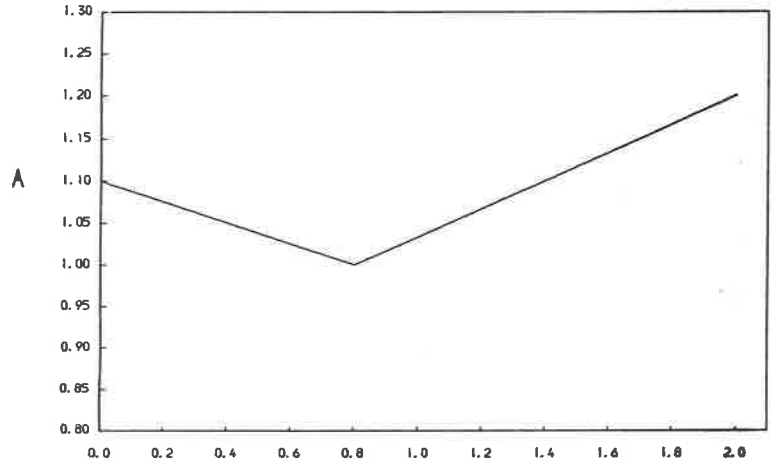

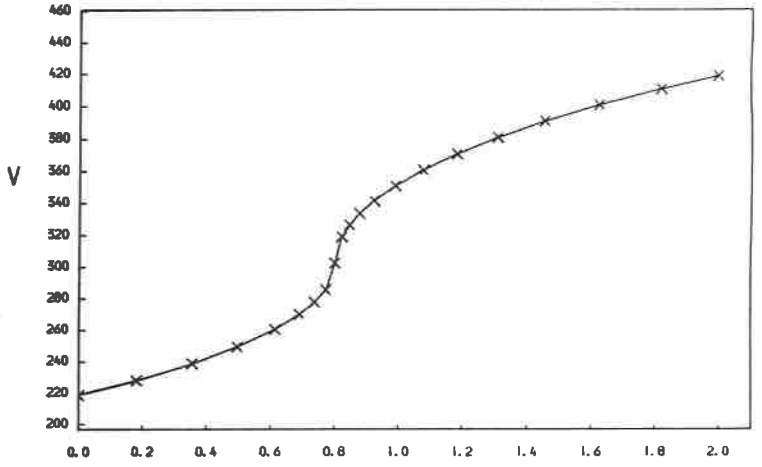

DE-LAVAL NOZZLE : TRANSITION FLOW

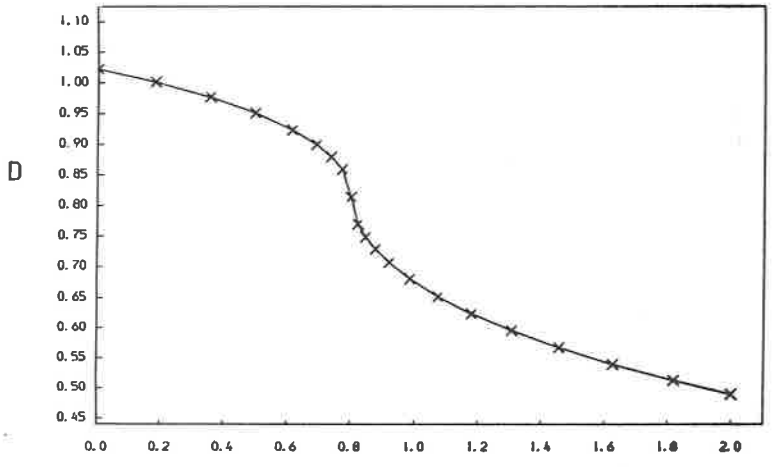

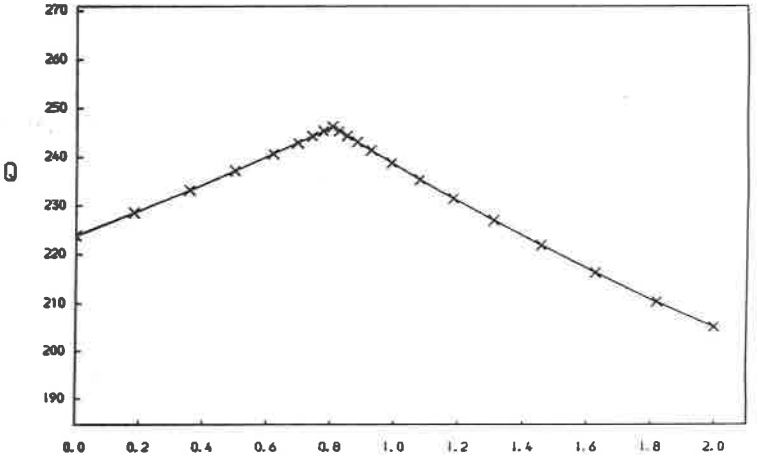

FIG ELEVEN

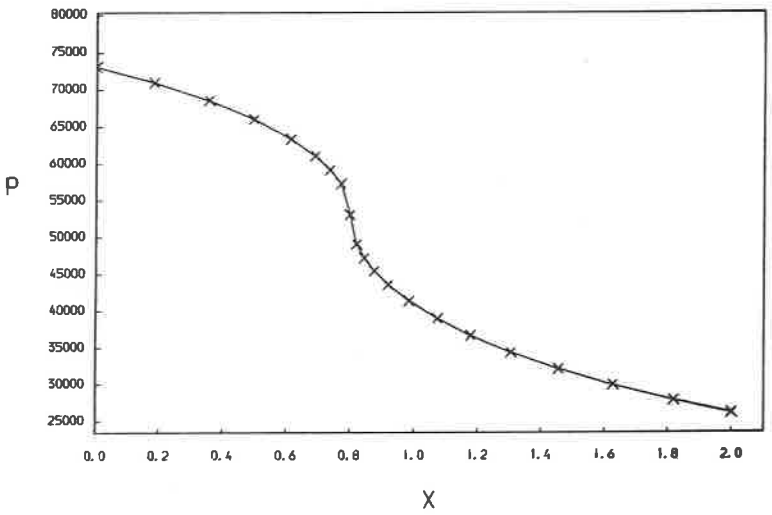

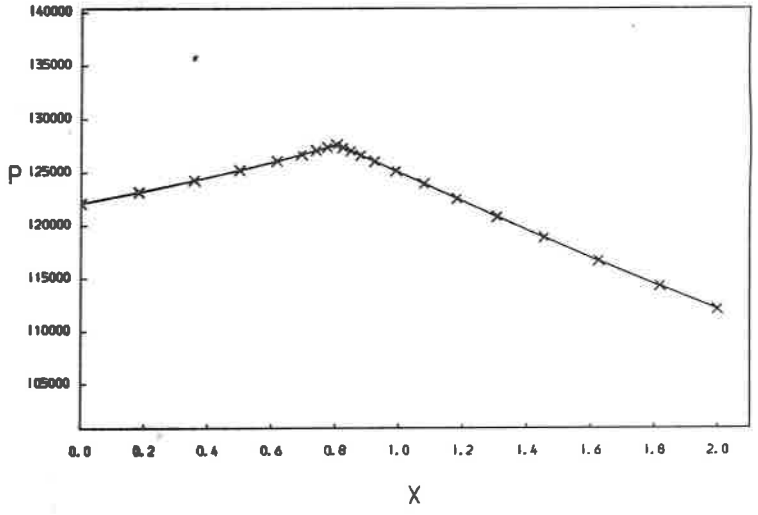

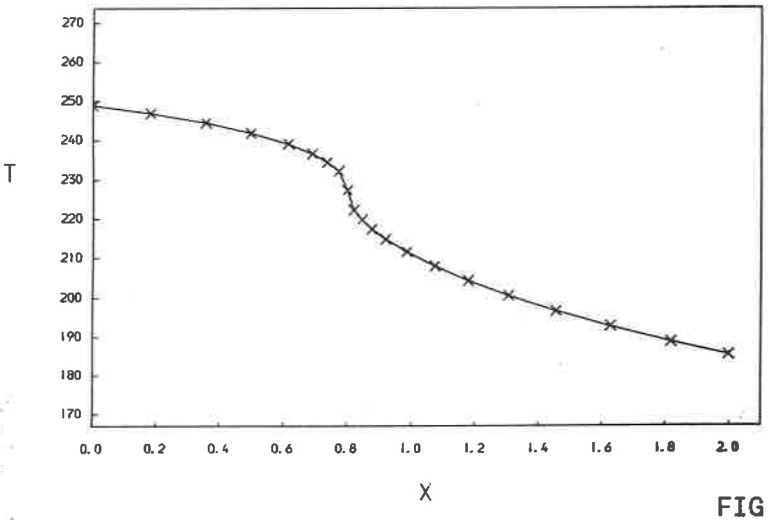

FIG ELEVEN

cont

CONCLUSION

A stationary principle has been constructed and used to determine an approximate finite element solution for quasi one-dimensional duct flow.

It is found that the numerical solution compares well with the exact solution (see [4]). A uniform grid may be used if a relatively small degree of curvature is present in the solution. Otherwise the accuracy decreases significantly unless a large number of nodes are employed in the formulation, this being computationally expensive. The accuracy may however be improved dramatically by the use of an appropriate fixed irregular grid.

There is clearly a need for an accurate, inexpensive, numerical method, not dependent on a-priori knowledge of the solution, which will generate an approximate solution automatically. In a subsequent report an adaptive grid formulation will therefore be considered.

REFERENCES

[1] COURANT, R. & FRIEDRICHS, K.O. : "Supersonic Flow And Shock Waves", INTER-SCIENCE, NEW YORK (1948).

[2] SEWELL, M.J. : "Maximum And Minimum Principles", CAMB. U. PRESS, CAMBRIDGE (1987).

[3] SEWELL, M.J. : "Properties Of A Streamline In Gas Flow", PHYS. TECHNOL. 16, (1985).

[4] WIXCEY, J.R. : "Compressible flow in ducts - analytic aspects", NUMER. ANAL. REPORT 12/88, DEPT. OF MATHS., UNIV. OF READING (1988).

[5] PORTER, D. & SEWELL, M.J. : "Constitutive Surfaces In Fluid Dynamics", DEPT. OF MATHS., UNIV. OF READING (1979).

[6] SEWELL, M.J. : "On Reciprocal Variational Principles For Perfect Fluids", J. MATHS. MECHS. 12, (1963).

[7] STRANG, G. & FIX, G.J. : "An Analysis of the Finite Element Method", PRENTICE-HALL, INC., ENGLEWOOD CLIFFS, N.J. (1973)

[8] CAREY, G.F. & DINH, H.T. : "Grading Functions and Mesh Redistribution", SIAM J. NUMER. ANAL. 22, (1985)